# Transferring functional chromosomes between intergeneric yeast generates monochromosomal hybrids with improved phenotypes and transcriptional responses

Transferring functional chromosomes between yeast

**Authors**

Yilin Lyu[1,2], Kunfeng Song[1,2], Jungang Zhou[1,2], Hao Chen[3], Xueying C. Li[4,*], Yao Yu[1,2,*]and Hong Lu[1,2]

**Affiliations**

[1] School of Life Sciences, State Key Laboratory of Genetic Engineering, Fudan University, Shanghai, China.

[2] Shanghai Engineering Research Center of Industrial Microorganisms, Shanghai, China.

[3] Personal Oncology Inc., Nanjing, Jiangsu Province, China.

[4] Ministry of Education Key Laboratory for Biodiversity Science and Ecological Engineering, College of Life Sciences, Beijing Normal University, Beijing, China.

[*] Corresponding authors. Emails: yaoyu@fudan.edu.cn; lixueying@bnu.edu.cn.

**Abstract**

Interspecific hybrids can exhibit phenotypes that surpass those of their parents, known as heterosis, which is often of interest for industrial applications and evolutionary genetics research. However, constructing hybrids between distantly related species, such as intergeneric yeasts, presents technical challenges. In this study, we established a method to transfer individual chromosomes from *Saccharomyces cerevisiae* (Sc) into *Kluyveromyces marxianus* (Km), an emerging model for bioproduction. The Sc chromosome of interest was circularized, genetically modified to carry Km centromeres and replication origins, and transformed into Km via protoplast transformation. With this method, we generated monochromosomal hybrids with eight Km chromosomes and Sc chromosome I or III. The Sc chromosomes exhibited normal replication, segregation, and active transcription in the hybrids. The hybrids displayed heterosis in flocculation and salt tolerance due to the overexpression of *FLO9* and *SPS22*, respectively. Transcriptomic analysis revealed that both *cis*- and *trans*-regulatory changes contributed to the divergence of gene expression between the two species, with the *cis* and *trans* effects often

acting in a compensatory manner. Our strategy has potential applications in optimizing cell factories, constructing synthetic genomes, and advancing evolutionary research.

**Teaser**

A yeast hybrid containing an alien chromosome transferred from a distantly related species exhibits improved phenotypes.

**MAIN TEXT**

## Introduction

The transfer of genetic materials between species is one of the major driving forces for speciation and environmental adaptation [1,2]. Chromosomes, which carry packs of genes, can introduce abundant genetic variation and contribute to evolution of adaptive traits when transferred between species. For example, horizontal transfer of plastid chromosomes between tobacco plants (*Nicotiana*) aided chloroplast capture [3]. Horizontal transfer of chromosomes between *Fusarium* species, a group of filamentous fungi, led to new pathogenic lineages [4]. Furthermore, hybridization is by nature a process of interspecific chromosome transfers. With the combined genetic materials, hybrids often exhibit enhanced phenotypes, known as heterosis or hybrid vigor. For example, hybridization between the top-fermenting yeast *Saccharomyces cerevisiae* and the cold-tolerant *S. eubayanus* gave rise to one of the most important lager-brewing species, *S. pastorianus* [5]. Similarly, triticale, a hybrid of rye (*Secale cereale*) and wheat (*Triticum aestivum L.*), exhibited improved yield in marginal environments [6]. Therefore, introduction of genetic materials from a distantly related species may hold great potential for phenotypic improvement in the fields of crop breeding and industrial applications.

Understanding the phenotypic and molecular consequences of interspecific hybridization may also address many important questions in genome evolution. For example, what are the molecular bases for heterosis [7]? From the perspective of gene regulation, can distantly related genomes regulate each other [8]? Is there an upper limit for evolutionary divergence such that two genomes with a divergence level above this threshold cannot regulate each other anymore? Is evolution of gene expression predominantly driven by *cis*- or *trans*-regulatory changes [9]? Many previous studies have addressed these questions with natural or synthetic hybrids [10–17], including important conclusions that sequence divergence in *cis*-regulatory elements such as promoters and

enhancers, as well as compensatory changes, became increasingly important for evolution of gene expression as evolutionary distance increases [16]. However, many of these questions remain open for distantly related species where natural hybrids are not available.

In this study, we explore the phenotypic and molecular consequences of hybridization between *Kluyveromyces marxianus* and *S. cerevisiae*, by synthetically constructing monochromosomal hybrids between the two distantly related species. *K. marxianus* is a yeast species that belongs to the *Saccharomycetaceae* family but only distantly related to *S. cerevisiae* (**Fig. 1A**). It has been previously argued that it may serve as an emerging model for bioproduction, including heterologous proteins, bioethanol and bulk chemicals [18,19]. It has a number of traits different from *S. cerevisiae*, including a high growth rate, thermotolerance, and the ability to assimilate a wide variety of sugars [20–22]. On the other hand, *S. cerevisiae* is more tolerant to ethanol than *K. marxianus* [19]. It is widely used in industrial fermentation and has arguably the best studied genome among eukaryotes [23]. Mixing the genetic materials between the two species is expected to provide novel phenotypes for industrial development, as well as to understand their evolution.

Stable allodiploid hybrids between the two species haven't been made available, although partial integration of *S. cerevisiae* genome fragments into *K. marxianus* has been achieved by protoplast fusion [24,25]. In order to introduce *S. cerevisiae* genetic materials in a systematic, controllable manner, we developed a genetic-engineering strategy to artificially transfer chromosomes between *K. marxianus* and *S. cerevisiae*. Artificial chromosome transfer was first established in 1977, when murine chromosomes were transferred into human cells via microcells [26]. To date, artificial transfer of functional chromosomes has primarily been achieved between closely related species (dashed lines, **Fig. 1B**), including transfers of human chromosome 21 into mouse and chicken cells [27–29], and between bacteria species *Mycoplasma mycoides* and *M. capricolum* [30]. *S. cerevisiae* (Sc) and *K. marxianus* (Km) diverged 114 million years ago [31], significantly exceeding the evolutionary distance between the species that have been shown capable of natural or artificial chromosome transfer (**Fig. 1B**). Previous efforts of protoplast fusion between Sc and Km showed that Sc genomes are often unstable after the fusion [25]. One possible explanation is the incompatibility of replicating elements such as centromere (*CEN*) and autonomously replicating sequence (*ARS*), as previously shown in hybrid incompatibility studies [32,33]. In this study, we engineered the Sc chromosome to resolve potential incompatibilities,

including circularization of the chromosome and insertion of *ARS* and *CEN* from the host species [34]. The engineered Sc chromosome was transformed into Km, creating a monochromosomal hybrid. Through phenotypic and gene expression analysis, we showed that functional chromosome transfer between distantly related species can produce beneficial phenotypes associated with overexpression of genes from the Sc chromosome. The transferred chromosomes triggered wide-spread transcriptional responses in the transferred and host genomes, suggesting cross-species regulation. Finally, we found that divergence of gene expression of the two species is often contributed by compensating *cis*- and *trans*-regulatory changes, providing new evidence for regulatory evolution across a long evolutionary timescale. Our strategy has potential applications in optimizing microbial cell factories and advancing evolutionary studies.

## Results

### Compatibility of ARS and CEN between Sc and Km

It is critical to ensure proper replication and segregation of the heterologous chromosome upon chromosome transfer. Therefore, we started by investigating the compatibility of *ARS* and *CEN* between Sc and Km. We examined transformation success and stability of plasmids carrying different combinations of *KmARS1*, *KmCEN5*, *ScARSH4* and *ScCEN6*. We found that *KmARS1* and *KmCEN5* was respectively essential for successful transformation (**Fig. 1C**, left**)** and plasmid maintenance in Km (**Fig. 1D**, left). Neither could be replaced by their Sc counterparts, *ScARSH4* and *ScCEN6*, suggesting incompatibility. Plasmids carrying *KmCEN5*+*KmARS1* produced transformants in Sc (**Fig. 1C**, right), but with poor stability (**Fig. 1D**, right), suggesting that *KmARS1* but not *KmCEN5* can function in Sc. Similar results were obtained using combinations of *KmARS18*, *KmCEN3*, *ScARS1* and *ScCEN4* (**Fig. S1**). The observed incompatibility could explain the rapid loss of Sc chromosomes in previous protoplast fusion between Km and Sc [25]. Finally, the plasmid containing both *ARS*s and *CEN*s from Sc and Km, known as double *CEN/ARS* plasmid, could replicate and segregate stably in both Km and Sc (**Fig. 1C**, left). Therefore, the issue of Sc chromosomal instability in Km may be resolved by engineering *KmCEN* and *KmARS* into Sc chromosomes.

Using double *CEN/ARS* plasmids carrying different antibiotic markers, we examined the mating rate between Km and Sc. We transformed haploid Km and Sc cells with plasmids carrying the $kan^R$ or $hyg^R$ marker, mixed them in different combinations (see **Methods**) and

selected for zygotes on double antibiotic medium (**Fig. 1E**). The results showed that the mating efficiency between Km *MAT***a** and *MAT*α cells, as well as between Sc *MAT***a** and *MAT*α cells, was around 16%. However, mixing $1.6\times10^7$ Km cells with $1.6\times10^6$ Sc cells, regardless of their mating types, failed to yield any zygotes, based on both double selection (**Fig. 1E**) and microscopic observation (**Fig. S2**). These results demonstrated a prezygotic reproductive barrier between the two species, which urges a synthetic method for generating Km-Sc hybrids.

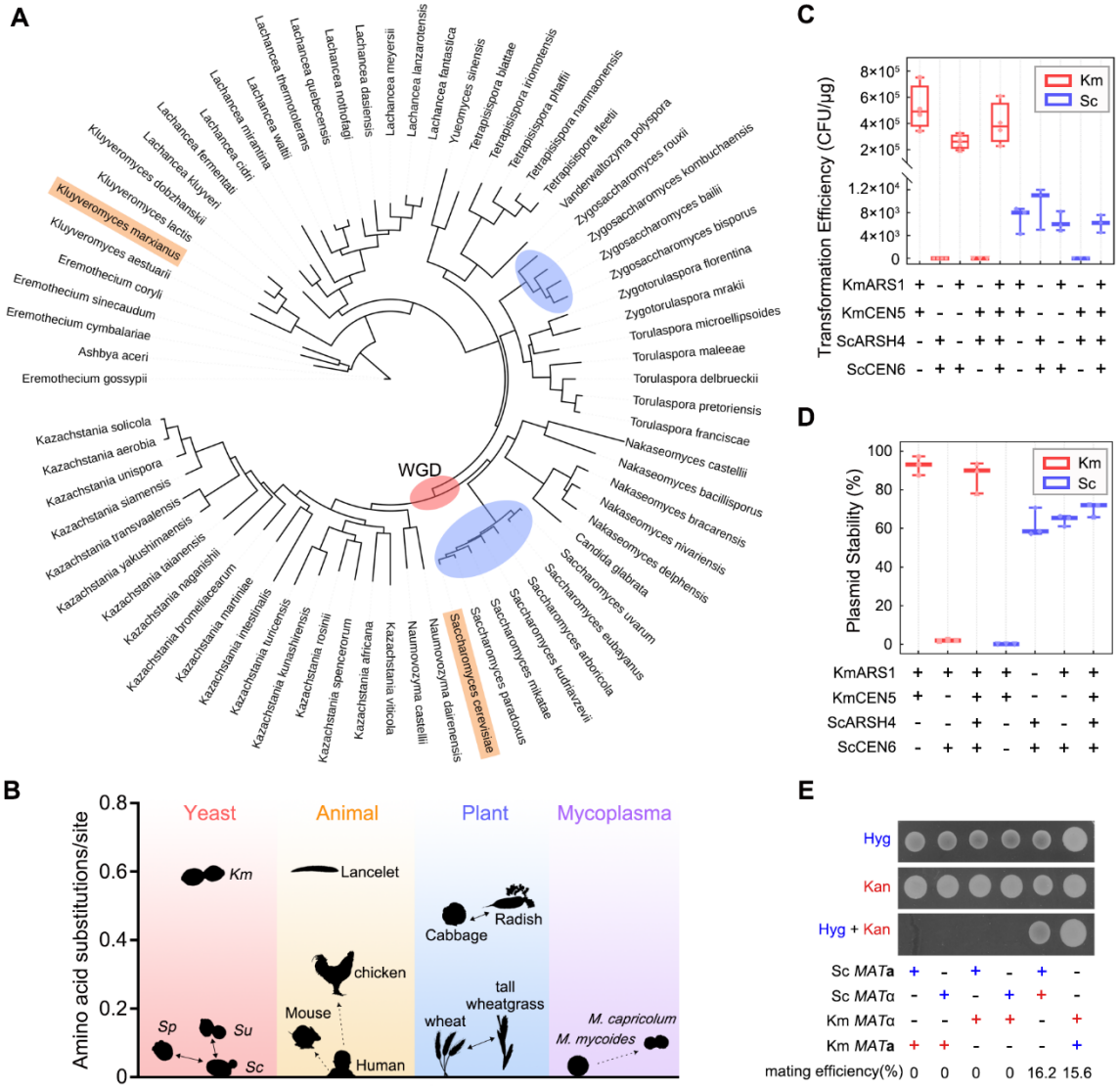


**Fig. 1. Functionality of ARS and CEN in Sc and Km. (A)** Phylogenetic tree of the *Saccharomycetaceae* family based on 71 selected species. Blue ellipses show species capable of interspecific hybridization, while red ellipse marks the event of whole-genome duplication. Sc and Km are highlighted in orange. The tree was constructed with iqtree2 [35] with concatenated coding sequences of 2,408 orthologous groups [31]. **(B)** The evolutionary distance between Km and Sc, compared to species in other taxa that are capable of interspecific hybridization (solid

lines) or tolerant to chromosomal transfer (dashed lines). Data of amino acid substitutions per site were generated by Orthofinder2 [36]. Sp, *Saccharomyces paradoxus*. Su, *S. uvarum*. **(C, D)** Transformation efficiency **(C)** and stability **(D)** of plasmids containing different combinations of *ARS* and *CEN* alleles in the two species (blue for Sc, red for Km). Stability refers to the percentage of cells containing the plasmid after being grown in non-selective YPD medium for 24 h. Lines in the boxplots and whiskers show the median, maximum and minimum values. **(E)** Mating assay between Km and Sc. Haploid Km or Sc cells containing a *kanR* (red cross) or *hygR* (blue cross) plasmid were mixed and spotted onto a medium containing hygromycin (Hyg), kanamycin (Kan), or both. Mating efficiency was quantified by counting double-resistant colonies (see **Methods**), represented by the mean of three replicate experiments.

## Engineering and transferring Sc chromosomes into Km

We selected the smallest Sc chromosome, chrI (chr1, 252 kb, 117 genes), and the third smallest chromosome, chrIII (chr3, 341 kb, 184 genes), for proof-of-principle experiments of Sc-Km chromosomal transfer. The experimental pipeline is shown in **Fig. 2A**. First, we circularized the chromosomes of interest to avoid potential incompatibility of telomeres. Sc telomeres (TELs) are composed of $TG_{1-3}$ repeat sequences, while Km TELs consist of a long repeat motif (25 nt) [37]. We removed the TELs from chr1 and chr3, respectively, and joined the ends with *KmURA3* with CRISPR/Cas9 [38]. To avoid homologous recombination at the telomeres, the telomere-associated long repetitive sequence on chr1 was deleted during circularization [38]. Next, to ensure stable maintenance of Sc chromosomes in Km, we inserted *KmCEN5 /ARS1* adjacent to the native *CEN*s on chr1 and chr3. Given that chr1 and chr3 contain 5 and 12 *ARS*s, respectively [39], we placed another copy of *KmARS1* close to a native *ScARS*, which was about ~100 kb away from the *KmCEN5 /ARS1* in the circular chromosomes (see **Methods** for details). The engineered circular chr1 and chr3 were named R1 and R3, respectively. Sc cells with R1 ("Sc-R1") or R3 ("Sc-R3") showed no fitness defect under normal culture conditions as well as in the presence of microtubule depolymerizing agents and DNA damage agents (**Fig. S3**), indicating that the introduction of *KmARS1* and *KmCEN5* did not affect chromosome replication in Sc. The circularization was confirmed by pulsed-field gel electrophoresis (PFGE), which showed an absence of linear chr1 or chr3 in the gel (**Fig. 2B**). Following a protocol developed by Noskov et al. [40], we extracted and column-purified R1 and R3, with the undesired linear chromosomes removed by exonuclease. Finally, the purified R1 and R3 were separately transformed into Km using protoplast transformation [41], yielding four R1 transformants (*Kluyveromyces-Saccharomyces*-R1, "KS-R1" hereafter) and one R3 transformant ("KS-R3"). The low number of

transformants indicates a need for further optimization of the transformation protocol, especially for transferring larger chromosomes.

We examined KS-R1 and KS-R3 for the integrity of the transferred chromosomes. All four KS-R1 transformants retained six Sc-specific markers located on R1 (**Fig. 2C**, see **Table S6** for marker positions), indicating successful transfer of R1. The transfer was further confirmed by restriction digest (**Fig. 2E**) and whole genome sequencing, which found no mutations in the transferred R1. In PCR analysis of KS-R3, marker 7 was absent (**Fig. 2D**, see **Table S6** for marker positions). PFGE analysis showed that the size of linearized R3 was smaller than the expected 340 kb (**Fig. 2E**). Genome sequencing revealed a 29 kb deletion between two direct repeats of putative Ty elements in R3 (**Figs. 2F & S4**). The deletion was potentially due to homologous recombination between Ty elements, the rate of which has been shown to significantly increase in circular plasmids during transformation [42]. The deleted region contained 13 genes (*MAK32*, *PET18*, *MAK31*, *HTL1*, *HSP30*, *YCR022C*, *YCR023C*, *SLM5*, *YCR024C-B*, *PMP1*, *YCR025C*, *NPP1*, *RHB1*). We introduced the deleted region, in six individual segments via plasmids, into Km cells (**Fig. S4**). None of the segments affected growth (**Fig. S4**), excluding the possibility that the loss of the 29 kb region was an adaptive response to overcome incompatibility.

We next evaluated the Km genome integrity after transformation. The PFGE patterns of Km chromosomes in KS-R1 and KS-R3 were consistent with the Km parent (**Fig. S5**). Genome sequencing revealed 33 mutations in 11 ORFs, as well as 82 SNPs and indels in intergenic sequences in Km chromosomes in KS-R1 (**Table S3**). The Km chromosomes in KS- R3 contained 4 mutations in 4 ORFs, and 47 SNPs and indels in intergenic sequences (**Table S3**). These mutations might have been induced during the protoplast transformation. Overall, the transfer of R1 or R3 into Km did not result in fusions, translocations, or other large-scale rearrangements in the Km chromosomes, thus creating a monochromosomal hybrid containing eight Km chromosomes and one Sc chromosome.

Subsequently, we examined the hybrids for any fitness defects. In rich medium (YPD), the growth curves of KS-R1 and KS-R3 were indistinguishable from Km-V, the parental Km strain with a void vector (**Fig. 2G**). Under non-selective conditions, R1 and R3 were highly stable in the hybrids. The loss rate per generation for R1 and R3 in YPD was 0.11% and 0.84%, respectively (**Fig. 2H**), a level comparable to that of circular YACs in Km [43]. Furthermore, KS-

R1 and KS-R3 exhibited robust growth in the presence of the microtubule depolymerizing agents benomyl (BML) and thiabendazole (TBZ), DNA replication inhibitor hydroxyurea (HU), the DNA-damaging agents methyl methane sulfonate (MMS) and camptothecin (CPT) [44], or protein synthesis inhibitor cycloheximide (CHX) (**Fig. 2I**). Taken together, the introduction of R1 and R3 did not affect the growth, chromosome segregation, DNA replication, or protein synthesis of the hybrids in rich medium. The Km cells were tolerant to the transplantation of Sc chromosomes, reflecting cellular plasticity.

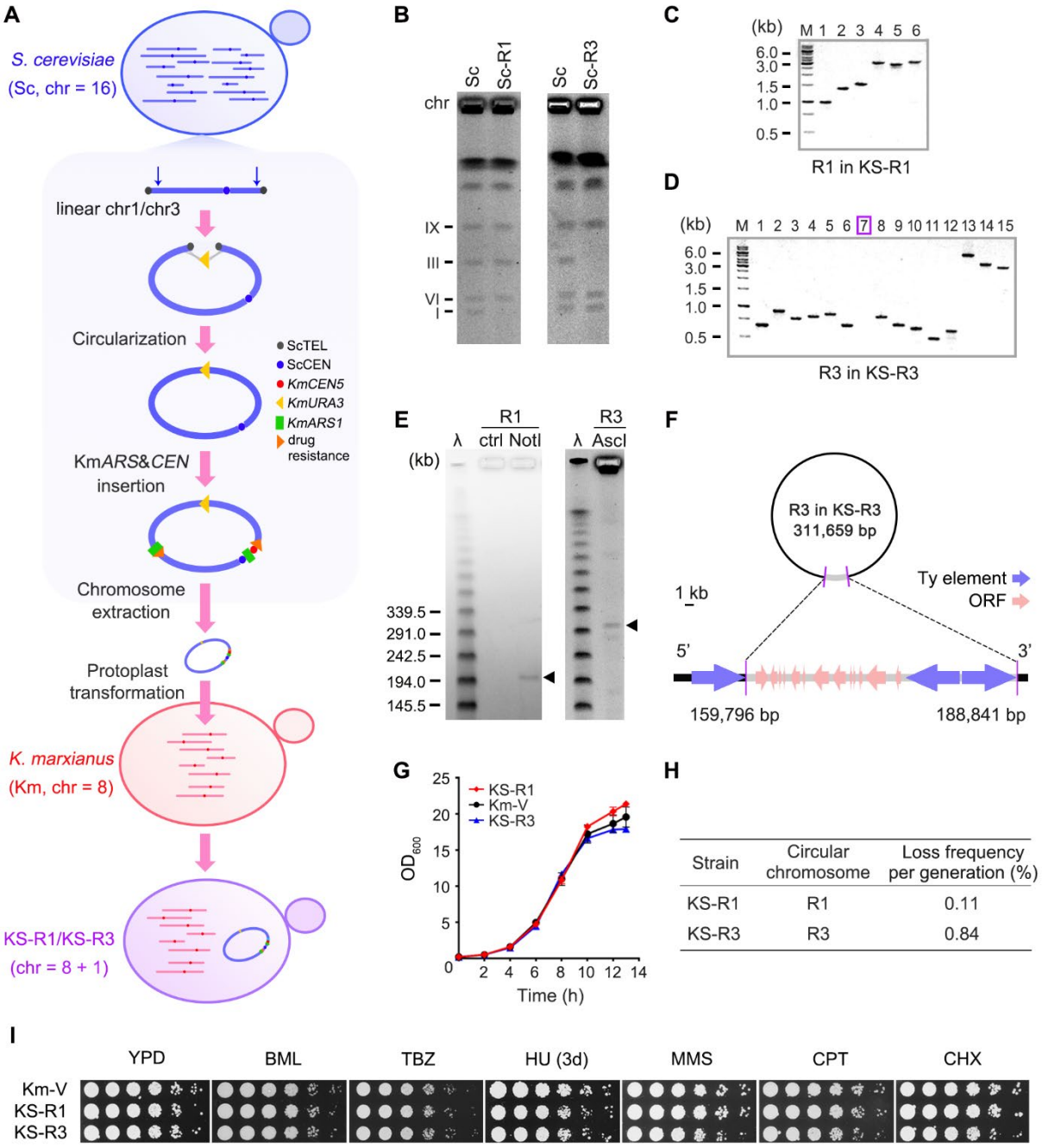


**Fig. 2. Engineering and Transferring Sc Chromosomes into Km. (A)** Experimental pipeline for transferring Sc chromosomes into Km. We used CRISPR technology to remove TELs (black points) from Sc chr1 or chr3 and connected the ends with the *KmURA3* marker (yellow triangle). We then inserted *KmCEN5*/*ARS1* (red points and green rectangles) and a drug resistance marker (orange triangles, $kan^R$ in chr1 and $hyg^R$ in chr3) near the endogenous *CEN* sequences (blue point). Another copy of *KmARS1* and a drug resistance marker ($hyg^R$ in chr1 and $kan^R$ in chr3) were placed close to a native *ScARS*. The circular chromosome was then extracted and transferred into Km via protoplast transformation, resulting in a monochromosomal hybrid containing eight Km chromosomes (red) and one Sc chromosome (blue). **(B)** PFGE of

chromosomal extracts from Sc-R1, Sc-R3 and the parental Sc strain. **(C, D)** PCR of markers in the circular chromosomes in KS-R1 **(C,** represented by one transformant**)** and KS-R3 **(D)**. Purple box labels the missing marker, #7, in KS-R3. See **Table S6** for marker positions. **(E)** PFGE of R1 and R3 (arrows) in the hybrids, linearized with NotI and AscI respectively. Ctrl: non-digested KS-R1 chromosomal extracts. λ: Lambda PFG Ladder. **(F)** Illustration of the 29 kb deletion in R3 of KS-R3. Coordinates are based on a manually curated R1 reference sequence (**Table S4**). **(G)** Growth curves of KS-R1, KS-R3, and Km-V in YPD. The values represent mean ± SD (n=3). **(H)** Stability of circular chromosomes in hybrids. The values represent the mean (n=3). **(I)** Spot assay of KS-R1 and KS-R3 in the presence of benomyl (BML), thiabendazole (TBZ), hydroxyurea (HU), methyl methane sulfonate (MMS), camptothecin (CPT) or cycloheximide (CHX). Unless otherwise indicated, the plates were incubated at 30 degrees for 1 day.

## Hybrids exhibit heterosis due to interactions between Km-encoded *trans*-factors and Sc *cis*-regulatory sequences

We next investigated if the transferred chromosomes conferred novel phenotypes. We treated the hybrids and their parents with twenty environmental conditions and semi-quantified their relative growth on solid media, using YPD growth as a reference (**Figs. 3A & S6**). The monochromosomal hybrids KS-R1 and KS-R3 exhibited comparable growth to Km-V under 19 and 15 conditions, respectively (**Fig. 3A**), suggesting that the small number of genes in R1 and R3 did not trigger a wide-spread metabolic reprogramming in Km. Under a few conditions, R1 and R3 caused growth defects, suggesting potential incompatibility. For instance, KS-R1 exhibited increased sensitivity to 42 ℃ and KS-R3 exhibited increased sensitivity to tunicamycin (TM) (**Fig. 3A-B**). The defective growth phenotypes were not shared by the two hybrids, indicating that the defects were caused by dominant effects of genes on R1 or R3, rather than a general effect caused by chromosomal transfers. Additionally, we ruled out the possibility that the mutations in the Km genome caused the phenotypes, because the strains no longer exhibited the phenotypes after losing the Sc chromosomes in non-selective medium (**Fig. S7**).

Interestingly, the chromosomal transfer resulted in heterosis. KS-R3 exhibited enhanced tolerance to high concentration of sodium chloride (NaCl) compared to its parents (**Fig. 3C**). The high-salt condition is a common stress in industrial processes. Therefore, increased tolerance to NaCl is a beneficial phenotype for industrial production [45]. We next investigated the molecular mechanisms by which R3 increased NaCl tolerance in the hybrid. Among the genes carried by R3, *ScSPS22* is involved in *β*-glucan synthesis and related to cell wall function [46]. In a previously published genome-wide screen, overexpressing *ScSPS22* reduced NaCl tolerance [47]. We thus tested if *ScSPS22* contributed to the enhanced NaCl tolerance of the hybrid. *ScSPS22*, along with

its 1000 bp upstream sequence (promoter), was introduced into Km via a centromeric plasmid. We found that, in contrast to its role in Sc, *ScSPS22* increased NaCl tolerance of Km to the same level as KS-R3 (**Fig. 3C**, upper panel). Expressing the Km ortholog of *ScSPS22*, *KmSPS22* (KLMA_10044), did not have an obvious effect (**Fig. 3C**, upper panel). This result indicates that *ScSPS22* is the causal gene for the increased NaCl tolerance in KS-R3. Additionally, overexpressing *ScSPS22* in Sc with centromeric or 2-micron plasmids reduced NaCl tolerance (**Fig. 3C**, lower panel), consistent with the previous report.

In order to understand the contribution of *cis*-regulatory and coding sequences (CDS) to the phenotypic effect of *ScSPS22*, we constructed a chimeric allele consisting of the promoter of *KmSPS22* and the CDS of *ScSPS22*, namely *Pkm-ScSPS22*. There was no substantial difference between *Pkm-ScSPS22* and *KmSPS22* when expressed with a centromeric plasmid (**Fig. 3C,** upper panel), suggesting a lack of functional divergence in the CDS. On the contrary, *Pkm-ScSPS22* conferred a much lower level of NaCl tolerance than *ScSPS22* driven by its endogenous promoter, indicating that the Sc promoter was causal for the increase in NaCl tolerance.

The different phenotypic effects of Sc and Km promoters suggest potential divergence in gene expression. Therefore, we analyzed the transcription level of *ScSPS22* and *KmSPS22* in the hybrid and parents by qPCR (**Fig. 3D**). The relative mRNA level of *ScSPS22* in KS-R3 was respectively 53 and 80 times higher than those in Sc-R3 with and without NaCl (**Fig. 3D**, right panel), suggesting that (1) a significant difference in *trans*-acting regulators for *ScSPS22* between Sc and KS-R3; and (2) the up-regulation of *ScSPS22* in KS-R3 is constitutive. The relative mRNA level of *KmSPS22* did not significantly differ between KS-R3 and Km-V (**Fig. 3D**, left panel), indicating little difference in the *trans*-acting factors for *KmSPS22* between Km and KS-R3.

When transformed into Km on a centromeric plasmid, the *ScSPS22* allele was expressed at the same level as *ScSPS22* in KS-R3 ($p > 0.05$ for both YPD and NaCl conditions, Student's t-test, **Fig. 3D**), suggesting that the promoter sequence of *ScSPS22* was causal for its up-regulation in KS-R3. The chimeric allele *Pkm-ScSPS22* drove much lower expression than *ScSPS22* in Km, consistent with *cis*-regulatory divergence. In Sc-R3 background, expressing *ScSPS22* with centromeric or high-copy 2μ plasmids increased its relative mRNA level, but failed to match the level of *ScSPS22* in KS-R3, suggesting that the upregulation of *ScSPS22* in KS-R3 resulted from induction or de-repression by Km-specific *trans*-acting factors, rather than increased gene copy

number. Taken together, the phenotypic and expression analysis showed that the heterosis in NaCl resistance was caused by specific interactions between Km-encoded *trans*-acting regulators and the Sc promoter of *SPS22*.

Although KS-R1 did not show any significant heterosis in the twenty conditions shown in **Fig. 3A**, we found that it exhibited a flocculation phenotype surpassing that of the parental Km-V and Sc-R1 (**Fig. 3E&F**). The flocculation phenotype disappeared after the loss of R1, indicating that R1 is responsible for the enhanced flocculation (**Fig. S8**). Flocculation facilitates cell sedimentation, reducing separation costs in high-density fermentation [48]. The *FLO* family genes control flocculation [49], among which *ScFLO9* is present on R1. Introducing *ScFLO9* with its 1000 bp upstream sequence into Km via a centromeric plasmid enhanced flocculation to the same level as KS-R1 (**Fig. 3E&F**). This result suggests that *ScFLO9* is responsible for the increased flocculation phenotype in KS-R1. Overexpressing *ScFLO9* with a centromeric or 2μ plasmid in Sc slightly enhanced flocculation (**Fig. 3E&F**), consistent with its known role in Sc but suggesting its effect is background dependent.

We similarly analyzed the expression level of *FLO9* to understand the molecular mechanisms of the heterosis phenotype. qPCR showed that the relative mRNA level of *ScFLO9* in KS-R1 was 64 times higher than in Sc-R1 (**Fig. 3G**), again suggesting a significant change in the *trans*-regulatory environment. The high expression in KS-R1 was recapitulated by *ScFLO9* expression from a centromeric plasmid in Km (light pink bars in **Fig. 3G**, $p > 0.05$, Student's t-test). The expression level of *KmFLO5* (KLMA_10835), the *ScFLO9* ortholog, was not increased in KS-R1, consistent with a lack of change in *trans* environment for Km genes (**Fig. 3G**, left panel). Overexpressing *ScFLO9* in Sc-R1 with centromeric and 2μ plasmids led to an increase in the mRNA level of *ScFLO9* expression (purple bars in **Fig. 3G**), with the higher level of $ScFLO9_{2\mu}$ correlating with faster flocculation (**Fig. 3F**). Taken together, the enhanced flocculation of KS-R1 was associated with *ScFLO9* being exposed to an alien *trans*-regulatory environment encoded by the Km genome. In both cases of *SPS22* and *FLO9*, the genetic combinations between Km-encoded *trans*-factors and Sc-encoded *cis*-factors would never be found in nature due to reproductive isolation, demonstrating the power of cross-species synthetic biology.

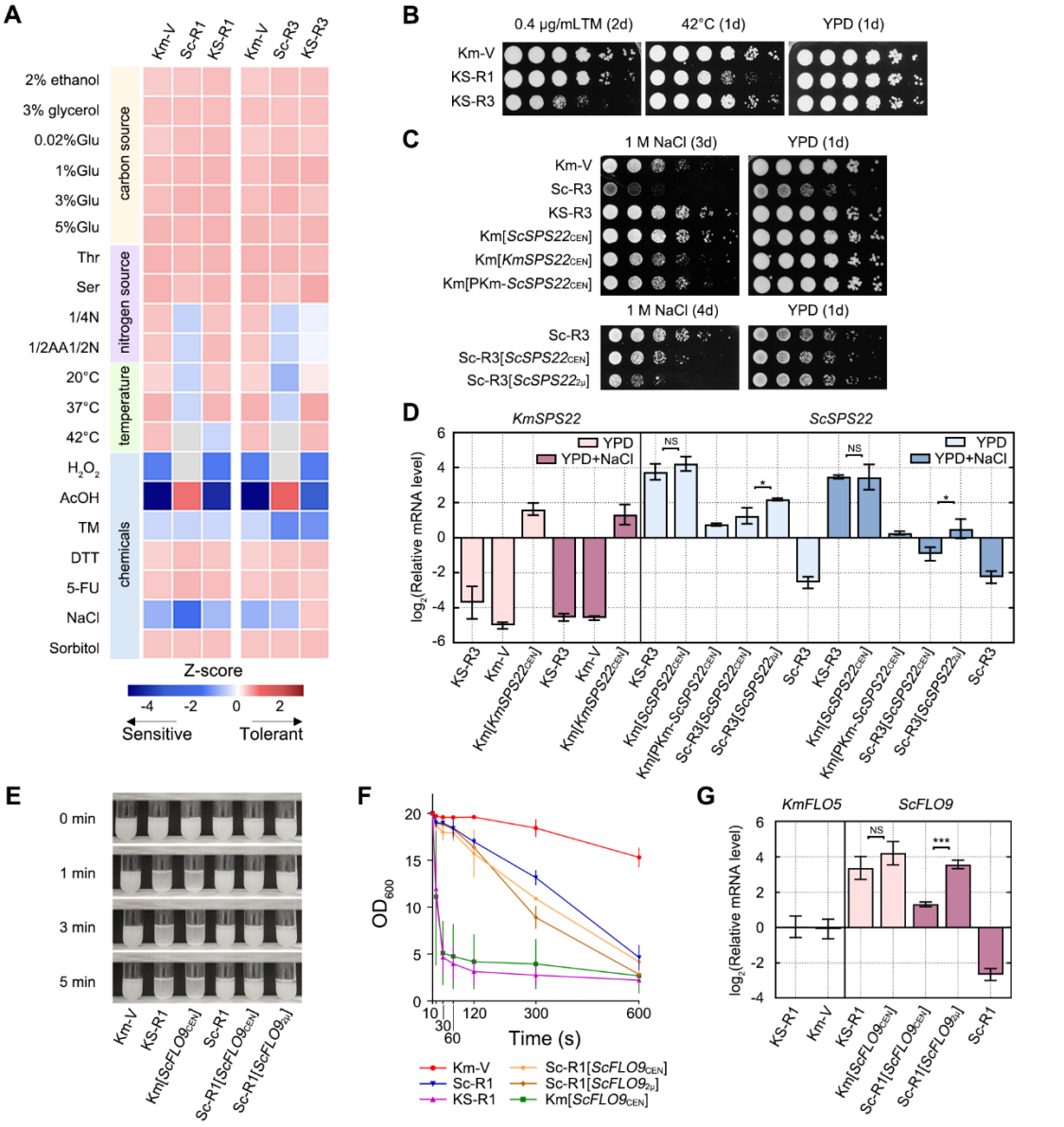


**Fig. 3. Hybrids exhibit heterosis. (A)** Growth phenotypes of hybrids and their parental strains under various conditions. Relative growth was semi-quantified through greyscale scanning of images from spot assays and normalized to YPD growth. Original images are provided in **Fig. S6**. The heatmap shows Z-scores of $\log_2$-transformed data. Grey denotes conditions where the strain could not grow. Glu, glucose; 1/4 N, one-quarter ammonium sulfate; 1/2 AA, half amino acids; 1/2 N, half ammonium sulfate; TM, tunicamycin; 5-FU, 5-fluorouracil. **(B)** Growth defects under tunicamycin or 42°C treatment associated with the transferred Sc chromosomes. **(C)** Improved NaCl tolerance associated with the promoter sequence of *ScSPS22*. *ScSPS22*, *KmSPS22* and *PKm-ScSPS22* alleles were expressed with a centromeric plasmid (indicated by the subscript CEN) or a 2μ plasmid (*ScSPS22*$_{2\mu}$) in either Km (upper panel) or Sc-R3 (lower panel). Serial dilutions were performed at 1:5 for all spot assays in this study. **(D)** Relative mRNA levels of *ScSPS22* and *KmSPS22* measured by qPCR. mRNA levels in the hybrid and Km cells were normalized to the average level of three housekeeping genes, *KmSWC4*,

*KmTRK1*, and *KmMPE1*. mRNA levels of *ScSPS22* in Sc were normalized to the average level of *ScSWC4*, *ScTRK1*, and *ScMPE1*. The values represent the mean ± SD (n=3). **(E, F)** Enhanced flocculation in KS-R1 associated with *ScFLO9*. *ScFLO9* was expressed with either a centromeric plasmid (*ScFLO9* $_{CEN}$) or a 2μ plasmid (*ScFLO9*$_{2\mu}$) in Km or Sc-R1. The strains were cultured overnight in SD-Ura or SD-Leu (see **Methods**) to an $OD_{600}$ of 20. The cultures were vortexed vigorously and left still, before being imaged **(E)** and examined for the $OD_{600}$ of the supernatant **(F)** at designated timepoints. The values in **(F)** represent the mean ± SD (n=3). **(G)** Relative expression levels of *ScFLO9* and *KmFLO5* measured by qPCR and normalized as described above. The values represent the mean ± SD (n=3). *, $p<0.05$; ***, $p<0.001$. NS, not significant. P-values were based on t-tests.

## Pervasive transcriptional responses triggered by chromosomal transfer

The experiments with *ScSPS22* and *ScFLO9* revealed significant changes in Sc gene expression after being transferred to Km. To determine if this is a general pattern, we analyzed transcriptomes of the hybrids (KS) and parental strains in YPD and under two stress conditions, 1 μg/mL tunicamycin (TM) and 1 M NaCl. All 89 genes on R1 and 151 genes on R3 (excluding those in the deleted 29 kb region and artificially inserted marker genes *KanR*, *hygR* and *KmURA3*) were actively transcribed in the hybrids under the three conditions (read counts >5) (**Table S4**). However, their expression in hybrids poorly correlated with that in Sc, with an average correlation coefficient ($R^2$) of 0.31 for R1 genes between Sc and KS expression, and an average of $R^2$ of 0.36 for R3 genes (**Fig. 4A**). This correlation was substantially lower than the correlation between the expression of human genes on Hsa21 transplanted into mouse cells and their counterparts in human cells ($R^2$=0.90) (21), which aligns with the remote evolutionary distance between Km and Sc (**Fig. 1B**). Compared to Sc, on average, 38.1% and 16.8% of the genes in R1 and R3, respectively, were up-regulated in KS, while 16.7% and 29.8% of the genes in R1 and R3 were down-regulated in KS, respectively (FDR-adjusted $p < 0.05$ by Wald test and absolute log2FoldChange >1; **Fig. 4B**). The median log2-fold change for up- and down-regulated genes was 2.06 and -1.67, respectively. Consistent with the case studies of *SPS22* and *FLO9*, the high proportion and fold change of differentially expressed Sc genes reflect dramatic differences in the *trans*-regulatory environment between Sc and the hybrids.

The Sc genes showing differential expression between Sc and hybrids were in general uniformly distributed across the transferred chromosomes (**Figs. 4C & S9**), but we found a region around *HML* that showed de-repression across multiple genes in KS-R3, providing an interesting example for chromatin-level regulatory divergence. The *HML* locus is flanked by

*GEX1* and *VBA3* on one side and *CHA1* on the other side (**Fig. 4D**). Notably, *GEX1* and *VBA3* were substantially upregulated in KS-R3 under all three conditions compared with those in Sc-R3, while the level of *CHA1* did not change significantly (**Figs. 4D & S9**). *GEX1* and *VBA3*, but not *CHA1*, are bound by the *SIR* complex that spreads from the *HML* locus in Sc [50]. This suggests de-repression of the *HML* locus in KS-R3. The α1 and α2 genes within *HML* were silenced in the *MATa* strain Sc-R3, with their RNAseq reads falling below the read-count threshold (see **Methods**). qPCR showed that the relative mRNA levels of α1 and α2 were upregulated 42-fold and 39-fold, respectively, in KS-R3 compared with Sc-R3 (**Fig. 4D**). The composition of silencers between *Kluyveromyces* and *Saccharomyces* differs significantly [51]. The silencer of *HML* in KS-R3 might not be able to recruit essential proteins such as Rap1 and ORC to the locus [52], contributing to the de-repression of α1 and α2, and flanking *GEX1* and *VBA3*.

While the expression of Sc genes underwent significant changes in the hybrids, R1 and R3 also profoundly affected the expression of Km genes. Out of 4,857 Km genes, 1,248 and 1,121 genes in KS-R1 and KS-R3, respectively, exhibited significant expression differences compared to Km-V in YPD (**Fig. 4E, Table S5**). R1 encodes a transcription factor, Oaf1, that regulates at least 97 Sc target genes [53]. Among the Km orthologs of the known Sc target genes (see **Methods** for ortholog assignment), 34 (42.5%) showed differential expression in KS-R1. R3 encodes four transcription factors regulating at least 305 Sc target genes [53], with 71 (35.9%) of their Km orthologs differentially expressed in KS-R3 (**Table S5**). This suggests that transcription factors encoded by R1 and R3 might directly alter gene expression in Km, but a large fraction of the observed transcriptional changes might be explained by indirect or uncharacterized regulation. Under TM and NaCl stresses, the number of differentially expressed genes was substantially lower than in YPD (**Fig. 4E**, **Table S5**). These results indicate that the heterologous chromosomes induced pervasive changes in expression of the endogenous genome, potentially via novel Sc-Km regulatory interactions. Interestingly, regulation from the Km genome became dominant under stress conditions, removing much of the effects associated with foreign chromosomes found in YPD.

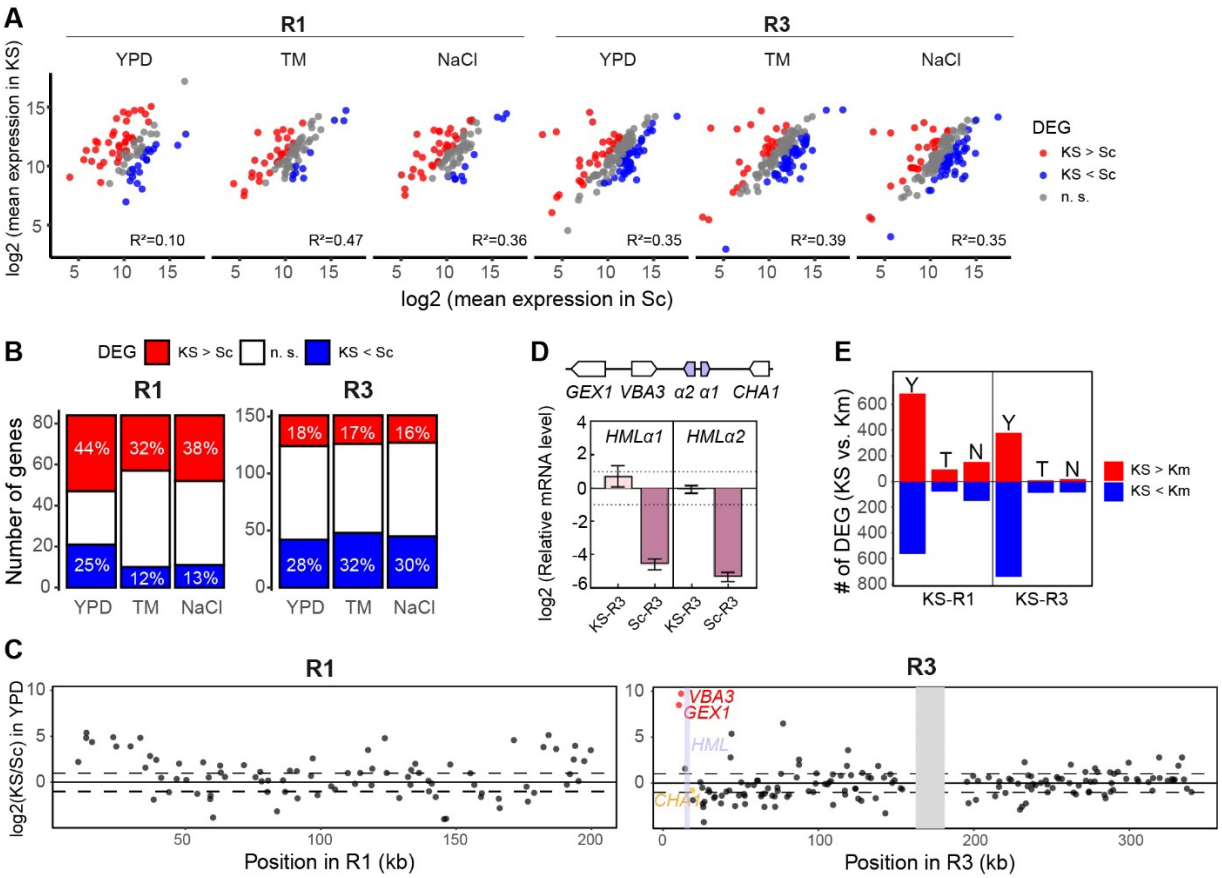


**Fig. 4. Transferred Sc chromosomes were actively transcribed in the hybrids. (A)** Correlation of gene expression between hybrids (KS) and Sc strains. The expression level was represented by log2 (average normalized read counts). Each point represents the average of three replicates. Adjusted $R^2$ were derived from linear regression. N = 84 genes for R1, and 151 genes for R3 (see **Methods** for data filters). DEG, differentially expressed genes. n.s., not significant. **(B)** Number of significantly up-regulated and down-regulated R1/R3 genes in hybrids. The number inside the column represents the percentage of up- or down-regulated genes. **(C)** Expression differences [log2(KS/Sc)] along R1 and R3 chromosomes in the hybrids in YPD. The gray shading indicates the deleted segment in KS-R3. Dashed lines indicate a log2FoldChange of 1 or -1. *VBA3* and *GEX1* are in red and *CHA1* is in orange. For stress conditions, see **Fig. S9**. **(D)** The relative mRNA levels of *HML*α1 and *HML*α2 in KS-R3 and Sc-R3 determined by qPCR. The mRNA levels were normalized to the average of three housekeeping genes as described in **Fig. 3D**. The values represent the mean ± SD (n=3). **(E)** Number of DEGs between KS strains and Km-V out of 4,857 Km genes. Y, YPD; T, TM; N, NaCl. In this figure, all DEGs are defined as an FDR-adjusted p-value < 0.05 by Wald test and abs(log2FoldChange) > 1.

## Contributions of *cis* and *trans* effects to the expression divergence between Km and Sc

The monochromosomal hybrids provide a unique opportunity to examine the contribution of *cis*- and *trans*-regulatory divergence to evolution of gene expression of the two remotely related species. In the hybrid, alleles from the two species are exposed to the same *trans*

environment, so their expression differences stem from differences in *cis*-acting regulatory elements, such as promoters, that are physically located on the same DNA strand of the regulated genes. The expression differences between the parental species are the sum of *cis*-and *trans*-acting effects, the latter being diffusible products (such as transcription factors) that are not linked with the affected genes (**Fig. 5A**) [9]. Studies on *Saccharomyces* and *Drosophila* hybrids indicate that expression divergence between species was mainly due to *cis* effects, while *trans* effects play a major role in transcriptional responses to environmental changes [11,54]. However, whether this tendency can explain the expression divergence between more distantly related species remains unresolved. Furthermore, in the cases where both *cis* and *trans* effects showed a significant contribution, it is often found that they act in a compensatory manner, consistent with stabilizing selection on gene expression.

In order to characterize the effects of *cis* and *trans* regulatory divergence, we identified Km orthologs for 70/89 genes on R1 and 112/151 genes on R3 (see **Methods**), with an average amino-acid sequence identity of 52.8% (**Table S7**). By comparing expression levels between alleles in the hybrids and parents, we identified genes with significant differential expression driven by *cis*-only, *trans*-only or *cis*-and-*trans* effects (see **Methods**; **Fig. 5B&C**). The genes were most commonly under both *cis* and *trans* effects (35-55%, **Fig. 5C**), which deviates from the previous notion that *cis* effects become increasingly dominant as species diverge [16]. However, we note that the pronounced *trans* effect could be associated with the fact that only one chromosome was transferred into the hybrids (see **Discussion**). Interestingly, when both significant, the *cis* and *trans* effects often act in the opposite direction, i.e. their effects compensate each other (green bars, **Fig. 5C**). Only a marginal proportion of genes showed reinforcing effects, where *cis* and *trans* effects act in the same direction (blue bars, **Fig. 5C**). This level of prevalence of compensatory effects suggests that stabilizing selection on gene expression might operate on a much longer evolutionary distance than previously appreciated.

Across environmental conditions, the correlations within *cis* effects (average correlation of 0.89) and *trans* effects (average correlation of 0.85) were high, indicating that the mechanisms causing gene expression divergence under different conditions are similar (**Fig. 5D**). Among the genes showing significant transcriptional responses to TM or NaCl treatment, genes with significant *trans* effects outnumbered those with *cis* effects (**Fig. 5E**). This highlights the major

role of *trans* effects in driving divergent expression responses under environmental stress, aligning with results from intragenus hybrids [11].

There were 44 (YPD), 60 (TM) and 57 (NaCl) genes that showed a conserved level of gene expression between Km and Sc, without any significant *cis* or *trans* effects. What factors could potentially drive their conservation? We considered (1) essentiality of genes and (2) the effect of gene duplication for this question. We found that the proportion of genes with conserved expression was slightly higher in essential genes compared to dispensable genes in all three conditions (**Figs. 5F and S10, Table S7**), although this trend was not statistically significant. After separating from Km, Sc underwent whole-genome duplication (WGD), leading to paralogs in Sc genome (**Fig. 1A, Table S7**). We found that the genes with paralogs were less likely to exhibit conserved expression than those without paralogs ($p = 0.03$ and 0.018 for YPD and TM conditions; $p = 0.23$ for the NaCl condition, Fisher's exact test; **Figs. 5F & S10**), consistent with the notion that gene duplication promotes functional divergence [55]. Among genes exhibiting regulatory divergence, the magnitude of *cis* effects in essential genes was significantly lower than in dispensable genes ($p < 0.001$, Student's t-test, **Fig. 5G**). The *cis* effects in genes without paralogs were significantly smaller than in genes with paralogs ($p < 0.05$, Student's t-test, **Fig. 5G**). In contrast, there was no significant difference in the magnitude of *trans* effects between essential and dispensable genes, nor between genes with or without paralogs (**Fig. 5G**). These findings suggest that the regulatory divergence in non-essential genes and paralogous genes could be partially driven by *cis*- but not *trans*-regulatory evolution [56].

Finally, we note that the monochromosomal hybrids' *trans* environment predominantly resembled Km, given that the transferred R1 and R3 chromosomes contained only a number of genes. As shown above, the pervasive expression changes in Sc genes upon chromosomal transfer reflected the divergence in *trans*-acting factors between Km and Sc. We expect that the change in *trans* environment would cause a more dramatic effect on Sc-specific genes that evolved after the split of the Sc and Km lineages. We identified 59 Sc-specific genes in R1 and R3, which did not have any identifiable orthologs in Km (**Table S7**). Indeed, the magnitude of expression differences between hybrids and Sc was significantly greater for Sc-specific genes than genes with orthologs ($p < 0.05$, Student's t-test; **Fig. 5H**). This potentially suggests that regulation of Sc-specific genes required co-evolution of *trans*-acting factors in a lineage-specific manner.

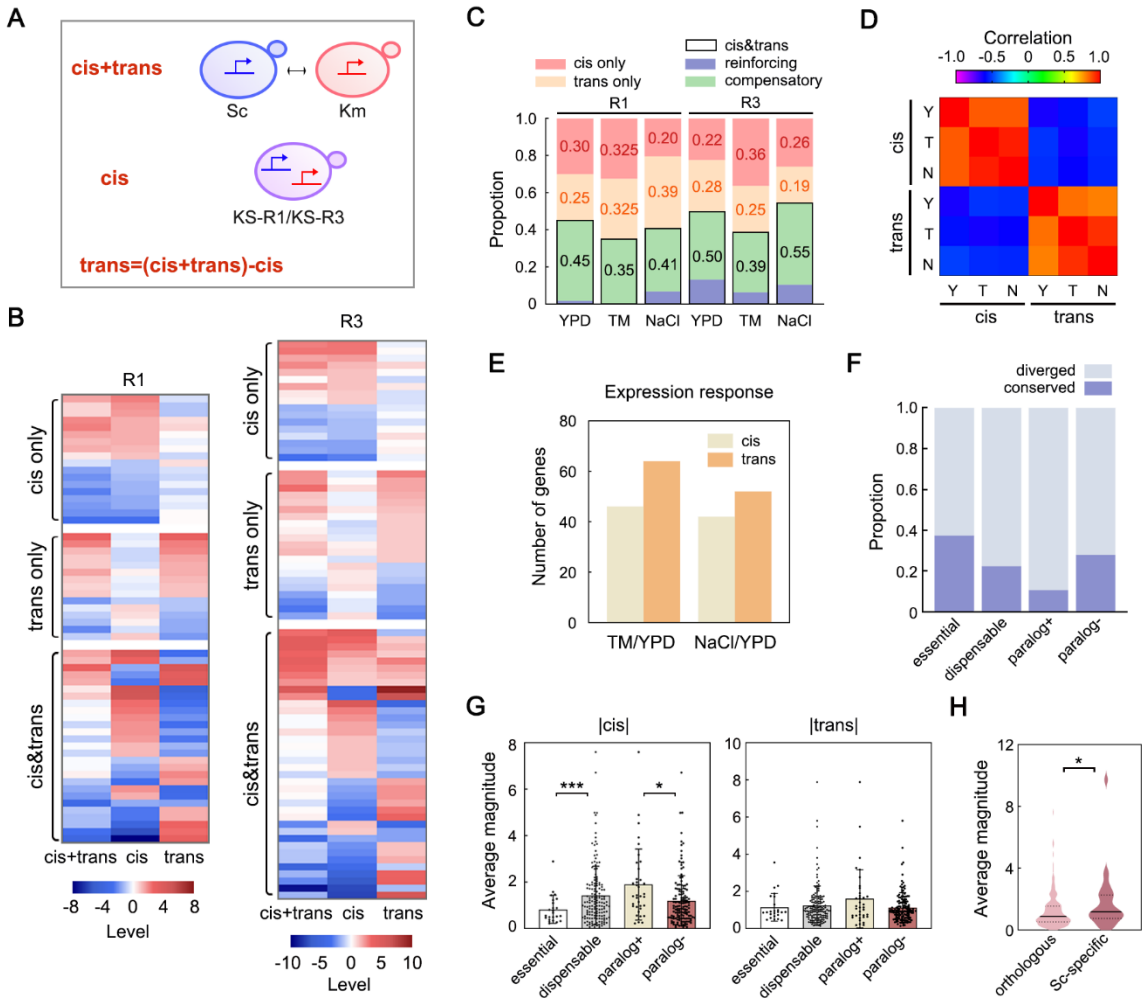


**Fig. 5. Contributions of *cis* and *trans* effects to the expression divergence between Km and Sc. (A)** Schematic representation of *cis* and *trans* effects in expression divergence between Km and Sc. The expression differences between Sc and Km reflect a combination of *cis* and *trans* effects (cis+trans). The expression differences between alleles in the hybrid reflect *cis* effects. Trans effects are calculated by subtracting *cis* effects from *cis*+*trans* effects. **(B)** Clustered heatmap of genes with only significant *cis* effects (*cis* only), only significant *trans* effects (*trans* only), or a combination of significant *cis* and *trans* effects (*cis* & *trans*) in YPD. **(C)** Proportion of genes showing *cis* only, *trans* only, *cis* & *trans*, compensatory (*cis* and *trans* effects act in the opposite directions), and reinforcing (*cis* and *trans* effects act in the same directions) effects in three conditions. Numbers indicate the proportion of *cis* only, *trans* only, and *cis* & *trans* category. **(D)** Genome-wide Pearson correlations between *cis* and *trans* effects across conditions. YPD (Y), TM (T), NaCl (N). **(E)** The number of genes with significant *cis* and *trans* effects among those showing the divergence of transcriptional response. **(F)** Proportion of genes exhibiting conserved and diverged regulation in YPD. For stress conditions, see **Fig. S10**. **(G)** The magnitude of *cis* and *trans* effects between essential and dispensable genes, and between genes with or without paralogs in Sc. The magnitude was represented by the average of the absolute values of *cis* or *trans* effects under three conditions. Bars and whiskers represent mean

494 ± SD. **(H)** The magnitude of expression differences in Sc-specific genes and orthologous genes.
495 The ratio between the expression level of a gene in the hybrid and that in Sc was calculated. The
496 magnitude was represented by the average of the absolute values of the log-transformed ratios
497 across three conditions. Values represent mean ± SD (n=3). P values in (G) and (H) were from
498 Student's t-test. *, $p<0.05$; ***, $p<0.001$.
499

500 **Discussion**

501 Interspecific hybridization often leads to novel phenotypes that are of interest for
502 industrial purposes and evolutionary studies. For diverged species that cannot mate naturally,
503 artificial chromosomal transfer provides an opportunity to explore the molecular and phenotypic
504 consequences of combining genetic materials evolved independently during millions of years of
505 evolution. In this study, we, for the first time, successfully introduced chromosomes of *S.*
506 *cerevisiae* to *K. marxianus*, two species both with great industrial potential but genetically as
507 diverged as human and lancelet (**Fig. 1B**). We show that the transferred Sc chromosomes are
508 stably maintained in Km. The monochromosomal hybrids exhibited heterosis, demonstrating the
509 technology's potential in future phenotypic screens. The improved salt resistance and
510 flocculation phenotypes were associated with Sc promoters being activated by Km-encoded
511 *trans*-acting factors in the artificial hybrids, to a greater level than the native regulation in Km or
512 Sc. Finally, we examined the molecular consequences of monochromosomal hybridization with
513 transcriptomic analysis, revealing broad transcriptional responses upon chromosomal transfer, as
514 well as prevalent compensatory evolution of *cis*- and *trans*-regulatory changes during the
515 divergence of the two species.

516 One of the technological advances in our study is the method to enable stable
517 maintenance of Sc chromosomes in Km. There are several technical factors of consideration.
518 First, we removed Sc TELs and circularized the chromosomes of interest. The circularization
519 made it possible to easily remove unwanted linear chromosomes by exonuclease treatment [40],
520 which may increase transformation efficiency. In the case of *CEN* engineering, it was important
521 to ensure that the heterologous *CEN* are not partially functional, which has been shown to disrupt
522 chromosome segregation and lead to dicentric breakage, thereby causing genome rearrangements
523 and instability [57]. We found that Sc and Km *CEN*s were non-functional in the other species.
524 Therefore, we may use double *CEN*s for maintaining the heterologous chromosomes. Next, we
525 considered the density of *ARS*s. The requirement of *ARS* density for YACs varied in previous
526 reports, from one *ARS* per 30 kb [58], 51 kb [59], to 1 Mb [60]. In our study, *KmARS1* was positioned at

a density of one *ARS* per 110 kb in R1 and 150 kb in R3, which proved to be sufficient for replication of Sc chromosomes in the hybrid. Finally, our strategy allows for possibilities of transferring multiple chromosomes into Km. This can be done either by marker recycling, i.e., popping out *URA3* in the monochromosomal hybrid (see the sequence design **File S1**) and transforming another chromosome subsequently, or by mating with another monochromosomal hybrid.

The synthetic Km-Sc monochromosomal hybrids showed interesting phenotypic and molecular characteristics, demonstrating that chromosome transfer is functional, even across a remote evolutionary distance such as between yeast genera. Previous interspecific chromosomal transfers in yeast have been successful in using *S. cerevisiae* as a container to maintain heterologous genetic materials from bacteria [30,60–62], but little interaction between the host and the heterologous chromosomes has been characterized, or desired at all. In our study, we found that the Sc chromosomes were "alive" in the Km background. All genes on the transferred R1 and R3 chromosomes were actively transcribed, despite a high level of sequence divergence. Genes on R1 and R3 showed significant expression differences between KS and Sc backgrounds, and the same for Km genes between KS and Km background. The transcriptional responses indicate active interspecific regulation, which can give rise to heterosis phenotypes, as shown with *SPS22* and *FLO9*. It is of future interest to investigate what proportion of the regulatory interactions between the two species' genomes are associated with beneficial phenotypes, or indicative of molecular incompatibility.

There are a few advantages in constructing functional monochromosomal hybrids for synthetic biology purposes. First, it partly circumvents the problem of genome incompatibility, which is a major barrier for hybridization between remotely related species. We found that, although Km and Sc cannot form hybrids, the monochromosomal hybrids with R1 or R3 were viable. It suggests that R1 and R3 did not carry incompatibilities that are detrimental to the hybrids' survival, although they may cause fitness defects under certain environmental conditions (**Fig. 3A**). These observations imply that R1 and R3 might carry environment-dependent incompatibilities, which should be noted in future studies. Second, the hybrids exhibited heterosis in a few phenotypes, demonstrating industrial potential. They also provide ideal materials for directed evolution for desirable traits, as demonstrated by other synthetic hybrids [63]. Third, the limited number of genes on transferred chromosomes made it easier to

identify the molecular basis of phenotypes of interest. We found that the flocculation phenotype in KS-R1 was due to overexpression of *ScFLO9*, consistent with its known role in Sc [64]. This suggests that the mechanism by which overexpressing *ScFLO9* boosts flocculation is conserved in both Sc and Km [64]. The heterosis in NaCl tolerance stems from overexpression of *ScSPS22* in KS-R3, which might be caused by loss of repressors [65]. It remains to be understood why overexpression of *ScSPS22* had an opposite effect in KS than Sc. One explanation lies in the different composition of glucan in cell wall between Km and Sc [66]. As a gene responsible for synthesizing *β*-1,3-glucan in the cell wall, *ScSPS22* might affect the two species differently under osmotic stresses.

The monochromosomal hybrids allowed for exploring evolutionary patterns of gene regulation between distantly related species. We found that the intergeneric expression differences were primarily driven by a combination of *cis* and *trans* effects (**Fig. 5B, C**), contrasting with previous findings with intrageneric species where expression divergence was mainly attributed to changes in *cis* effects [11,16]. However, we note that the monochromosomal hybrids differ from allodiploid hybrids in that its *trans* environment closely resembles one of the parental species (Km in this case). Therefore, the Sc and Km alleles experienced imbalanced changes in *trans* environment and the contribution of *trans* effects might be overestimated. In fact, the monochromosomal hybrids resembles introgression lines where only parts of the genomes are hybridized [67,68]. With this deviation in mind, our conclusion is consistent with analysis from 230 transgenic experiments on insects and nematodes, which suggests that *cis*-*trans* coevolution is more likely to accumulate over greater evolutionary timespans than *cis* or *trans* effects alone [69] . Another interesting finding is the prevalence of compensatory effects of *cis* and *trans* changes (**Fig. 5C**) [11,16]. It has been proposed that stabilizing selection acts to maintain gene expression, so the *cis*- and *trans*-acting changes might accumulate opposite effects. However, few studies have demonstrated that stabilizing selection on gene expression operates on such a long evolutionary timescale as Km and Sc. Finally, our study sheds light on evolutionary patterns that are difficult to study with intragenus hybrids, including the regulatory dynamics of paralogs and species-specific genes (**Fig. 5G, H**).

In summary, our study established a strategy for engineering the structural elements and ARS of a functional chromosome before transferring it between intergeneric yeasts. This strategy might be extended to other microbes as well as to plants. The resultant hybrids, containing

rationally designed synthetic genomes, provide valuable resources for cell factories, synthetic biology, and evolutionary genomics.

## Materials and Methods

### Strains and media

Yeast strains used in this study are listed in **Table S1**. Sc strain W303-1A (*MATa leu2-3,112 trp1-1 can1-100 ura3-1 ade2-1 his3-11,15*) was subjected to chromosome engineering. The engineered Sc chromosome was transferred into a *ura3Δ* Km strain, FIM-1ΔU [70]. The following media were used in this study: YPD [71], supplemented synthetic medium lacking uracil or leucine (SD-Ura or SD-Leu) (0.17% yeast nitrogen base without amino acids and ammonium sulfate, 2% glucose, 1 g/L sodium glutamate, 2 g/L DO Supplement-Ura (630416, Takara) or DO Supplement-Leu (630414, Takara), 2% agar for plates), SD (same recipe as SD-Ura, with the addition of 20 mg/L uracil), and ME (2% malt extract, 3% agar). G418 (A600958, Sango) and hygromycin (H8080, Solarbio) were added to YPD medium at final concentrations of 200 mg/L and 300 mg/L, respectively, to prepare YPDG and YPDH media. Both antibiotics were supplemented into YPD and SD-Ura to prepare YPDGH and SD-Ura+GH, respectively. Unless indicated, cells were grown at 30 ℃.

### Plasmids

All plasmids used in this study are listed in **Table S2**. All primers are listed in **Table S6**. A previously published vector LHZ626 which contains CEN and ARS elements from both Sc and Km (double CEN/ARS plasmid), as well as *KmURA3*, served as a control for circular chromosomes [41]. To construct plasmids for diploid selection, a fragment containing *ScARSH4* and *ScCEN6* was amplified from LHZ626 and inserted into the HpaI and SpeI sites of a Km-centromeric plasmid, LHZ882 [72], yielding LHZ1493. KANMX6 ($kan^R$) was amplified from pFA6a-KANMX6 and used to replace HPHMX4 ($hyg^R$) in LHZ1493 to produce LHZ1494. To create plasmids with different combinations of ARS and CEN from Km and Sc, a BamHI site was introduced between *KmARS1* and *KmCEN5* of LHZ882 to generate LHZ1495. *ScCEN6* was inserted between the BamHI and SalI sites of LHZ1495 to generate LHZ1496. *ScARSH4* was inserted between the BamHI and HindIII sites of LHZ1495 to generate LHZ1497. *ScARSH4* and *ScCEN6* were inserted between the HindIII and SalI sites of LHZ1495 to obtain LHZ1498.

In order to remove the telomeres and join the chromosomal ends, we first constructed CRISPR plasmids expressing single guide RNAs (gRNAs) targeting telomeres of each end of chr1 and chr3. Primers containing a 20 bp gRNA sequence were annealed in pairs and inserted into the SapI sites of pRS425-Cas9-2xSapI, resulting in plasmids LHZ1499A, B, LHZ1500A and B. Next, the gRNA cassette from LHZ1499A was inserted into the NotI site of LHZ1499B to produce LHZ1499. Similarly, the gRNA cassette from LHZ1500A was inserted into the NotI site of LHZ1500B to produce LHZ1500. The double-gRNA plasmids, LHZ1499 and LHZ1500, were subsequently transformed into yeast (see below). In order to insert *KmARS1* and *KmCEN5* into the circularized chromosomes, we cloned gDNAs into the SapI sites of pRS425-Cas9-2xSapI to construct LHZ1501~1504, following the same cloning procedure as described above. The homologous repair templates ("donor DNA", see below) used in CRISPR/Cas9 genome editing was assembled into pMD-18T with In-Fusion Snap Assembly (Clontech), according to the designs in **File S1**.

For flocculation analysis, the *ScFLO9* cassette, including 1000 bp upstream, the ORF of *ScFLO9*, and 200 bp downstream sequence was amplified from the genome of W303-1A. This cassette was inserted into the NotI site of LHZ626 to produce LHZ1505, and into the SmaI and SpeI sites of pRS315 and pRS425 to produce LHZ1509 and LHZ1510, respectively.

For NaCl tolerance analysis, the *ScSPS22* cassette, including 1000 bp upstream sequence, the ORF of *ScSPS22*, and 200 bp downstream sequence was amplified from the genome of W303-1A. This cassette was inserted into the NotI site of LHZ626 to produce LHZ1506, and into the SmaI and SpeI sites of pRS315 and pRS425 to produce LHZ1511 and 1512, respectively. The 1000 bp upstream sequence of *ScSPS22* in LHZ1506 was replaced by the 1000 bp upstream sequence of *KmSPS22* to produce LHZ1507. The *KmSPS22* cassette, including 1000 bp upstream sequence, the ORF of *KmSPS22*, and 200 bp downstream sequence was amplified from the genome of FIM-1ΔU and inserted into the NotI site of LHZ626 to produce LHZ1508. The full sequences of LHZ626, LHZ1495, and pRS425-Cas9-2xSapI are listed in **Table S2**.

**Transformation efficiency and stability of the plasmid containing different combinations of ARS and CEN from Km and Sc.**

Fim-1ΔU and W303-1A were grown in YPD liquid medium overnight. Cells from 1 mL-culture were pelleted and transformed with LHZ626, LHZ1495~LHZ1498, respectively, using

the lithium acetate (LiAc) method [73,74]. The cells were diluted and spread onto YPDH plates. Colony-forming units (CFUs) were counted after 3 days. The transformation efficiency (CFUs/μg DNA) was calculated taking the dilution factor into account. To measure the stability of the plasmid, transformants were grown in YPD liquid medium for 24 h. The cells were then diluted and spread onto YPD and YPDH plates. Stability was determined by dividing the CFU count on YPDH plates by that on YPD plates. The experiments were replicated three times.

**Mating assay**

The quantitative mating assay was performed as previously described [75] with modifications. Strains transformed with LHZ1493 (*hyg*$^R$) were used as experimental cells, and strains transformed with LHZ1494 (*kan*$^R$) served as tester cells. Both experimental and tester cells were cultured overnight in YPDH and YPDG liquid media, respectively. Cells were then washed and resuspended in $H_2O$ to an $OD_{600}$ of 1. A total of 100 μL of experimental cells was mixed with 500 μL of tester cells. The mixture resulted in a 1:5 ratio of experimental to tester cells when both cell types were Km or Sc. The mixture resulted in a 1:10 ratio of Sc experimental cells to Km tester cells, as CFU per $OD_{600}$ of Km cells was twice that of Sc cells. The mixed cells were pelleted, resuspended in 20 μL of $ddH_2O$, and spotted onto ME plates. After incubation at 30 ℃ for 24 h, cells were washed off the ME plates with $ddH_2O$ and then pelleted and resuspended in 1 mL of $ddH_2O$. To visualize the mating result, a total of 3 μL cells were spotted on YPDH, YPDG, and YPDGH (Fig.1E). These plates were incubated at 30 ℃ for 24 h. To quantify mating efficiency, the cells were diluted and plated onto YPD and YPDGH plates. The mating efficiency was calculated as the number of colonies on YPDGH plates divided by one-sixth of the number on YPD plates, reflecting the 1:5 ratio of experimental to tester cells. The experiments were replicated three times.

**Engineering of Sc chromosome I and III**

Each step of engineering Sc chromosome I (chr1) or III (chr3) involved transforming a CRISPR plasmid (**Table S2**) and a donor, which is a PCR product for homologous recombination repair. The composition and full sequences of the donors are listed in **File S1**.

Chr1 and chr3 were circularized as previously described [76]. First, LHZ1499 or LHZ1500 was transformed into W303-1A to induce double strand breaks in both telomeres in chr1 or chr3. A DNA fragment “chr1-cir” or “chr3-cir” containing *KmURA3* with homologous arms to the chromosomal ends was simultaneously transformed to connect the two chromosomal ends with

*KmURA3*. The constructs above were designed to remove the left telomere (0-1111 bp) and the right telomere along with the repetitive sequence (208917-252221 bp) of chr1, and the left telomere (0-831 bp) and the right telomere (334198-341087 bp) of chr3. Successful circularization was selected by SD-Ura-Leu medium. The transformants with circularized chromosomes were named Sc-ring1 and Sc-ring3.

In order to insert *KmARS1* and *KmCEN5* into the circularized chromosomes, we transformed LHZ1501 and a donor "chr1-ARS1" into Sc-ring1 to insert *KmARS1* and $hyg^R$ at 66090 bp of chr1, resulting in a strain named Sc-ring1L. LHZ1502 and a donor "chr1-ARS1/CEN5" were transformed into Sc-ring1L to insert *KmARS1*/*KmCEN5* and $kan^R$ at 157346 bp of chr1, resulting in a strain named Sc-R1. Similarly, LHZ1503 and a donor "chr3-ARS1/CEN5" were transformed into Sc-ring3 to insert *KmARS1*/*KmCEN5* and $hyg^R$ at 108718 bp of chr3, resulting in a strain named Sc-ring3L. LHZ1504 and a donor "chr3-ARS1" were transformed into Sc-ring3L to insert *KmARS1* and $kan^R$ at 243183 bp of chr3, resulting in a strain named Sc-R3. All transformations described above followed the LiAc method [73,74].

**Extraction and protoplast transformation of R1 and R3**

R1 and R3 were extracted from Sc-R1 and Sc-R3 as previously described [40], which was developed for purifying yeast artificial chromosomes up to 600 kb in size. A total of 10 μL R1 or R3 was transformed into Km by protoplast transformation [42]. The transformants were selected on SD-Ura+GH plates.

**Pulsed-Field Gel Electrophoresis (PFGE)**

Plugs containing the genome of Sc, Km, and hybrid cells were prepared by using the CHEF Yeast Genomic DNA Plug Kit (170-3593, Biorad). To separate circular R1 from linear chromosomes in KS-R1, chromosomes were separated on the CHEF MAPPER$^{TM}$ XA System in a 1% pulsed field certified agarose gel (162-0137, Biorad) in 0.5×TBE (diluted from 10×TBE, T1051, Solarbio) at 14 ℃. The running time was 24 h at 6.0 V $cm^{-1}$, with a 60~120 sec switch time ramp at an included angle of 120 °. The plug containing the entrapped R1 was cut out and linearized with NotI as described in the protocol of the CHEF Yeast Genomic DNA Plug Kit. Similarly, R3 in KS-R3 was separated from linear chromosomes and then linearized with AscI. Chromosomes of W303-1A, Sc-R1, Sc-R3, linearized R1 and R3 were separated in a 1% pulsed field certified agarose gel in 0.5×TBE at 14 ℃. The running time was 16 h at 6.7 V $cm^{-1}$, with a

10~40 sec switch time ramp at an included angle of 120 °. Lambda PFG Ladder (N0341S, NEB) was used as a size marker for PFGE.

**Growth curves of KS-R1 and KS-R3 and the stabilities of transferred chromosomes**

As a control, Fim-1ΔU was transformed with LHZ626 to produce Km-V. KS-R1, KS-R3, and Km-V were cultured in YPDGH liquid medium overnight. The overnight culture (referred to as day 0 culture) was diluted into YPD liquid medium to an initial $OD_{600}$ of 0.2 and grown at 30 ℃. To monitor growth curves, the $OD_{600}$ of the culture was recorded every 2 hours for the first 14 hours. To assess the stability of the transferred chromosomes, the culture was diluted into fresh YPD medium to start at an $OD_{600}$ of 0.2 every 24 hours, a period corresponding to approximately 7 generations. Cultures from day 0 and after 5 days of growth were diluted and plated onto YPD and YPDGH plates on the day the cultures were collected. Stability was determined by dividing the CFU count on YPDGH plates by that on YPD plates. The loss rate of transferred chromosomes per generation was calculated as previously described [72]. The experiments were replicated three times.

**Genome Sequencing**

Km-V, Sc-R1, Sc-R3, KS-R1, and KS-R3 were cultured overnight in SD-Ura+GH liquid medium. The cultures were diluted to an $OD_{600}$ of 0.2 and cultured until the $OD_{600}$ reached 0.6. The cells were collected and washed once with $ddH_2O$. Genomic DNA was extracted using the E.Z.N.A. Fungal DNA Kit (D3390, OMEGA Bio-Tek) and sequenced on the Illumina NovaSeq 6000 platform using the 150-bp pair-end sequencing strategy (BIOZERON, Shanghai, China).

To construct the reference sequences for R1 and R3, sequences of chr1 and chr3 were extracted from the W303-1A genome (GenBank assembly: GCA_002163515.1). We then manually modified the sequences to reflect our genome edits, including the insertions of Km elements and deletions of telomere sequences, giving rise to reference sequences R1 and R3 (provided in **Table S4**). Annotations for R1 and R3 were transferred from S288c annotations with SnapGene. The whole-genome sequencing data were processed by BIOZERON biotechnology. To identify *de novo* variants during circular chromosome transfer, the raw sequencing data of Sc and KS strains were aligned to reference sequences for R1 or R3 using BWA [77] with default settings. Picard tools were used to remove PCR duplicates. The average sequencing depth of KS-R1, Sc-R1, KS-R3, and Sc-R3 was 298, 1,183, 1,241 and 1,134 for the respective R1 or R3 chromosome. SNPs and indels were called following the best practices of

GATK HaplotypeCaller [78]. Then, all heterozygous variants were removed from the VCF files of KS-R1 and KS-R3. All variants coexisting in both KS-R1 and Sc-R1 or KS-R3 and Sc-R3 were filtered out from the KS-R1 and KS-R3 VCF files as well. The remaining variants were considered to have occurred during the chromosome transfer. In the case of R1, no *de novo* mutation was found.

To identify variants in the genome of Km, raw sequencing data of KS-R1, KS-R3, and Km-V were aligned to the reference genome of FIM1 (GenBank assembly: GCA_001854445.2) [79] combined with either R1 or R3 sequence, using BWA with default parameters. Picard tools were used to remove PCR duplicates. The average sequencing depth for KS-R1, KS-R3 and Km-V was 1,036, 1,102 and 615, respectively. GATK HaplotypeCaller was used to identify the variants in these strains, following its best practices. VCFtools [80] was used to remove variants shared between Km-V and KS-R1 or KS-R3, as well as heterozygous calls. The remaining unique, homozygous variants in KS-R1 and KS-R3 were listed in **Table S3**.

**RNAseq and qPCR**

Three biological replicates of Km-V, Sc-R1, Sc-R3, KS-R1, and KS-R3 were cultured overnight in SD-Ura+GH liquid medium. The cultures were diluted into YPD to achieve an $OD_{600}$ of 0.2. Once the $OD_{600}$ of the cultures reached 0.6, cells were collected directly for the YPD group. For stress treatment, the culture was supplemented with tunicamycin (T8480, Solarbio) at a final concentration of 1 μg/mL, or with NaCl at a final concentration of 1 M, and cells were collected after 1 hour. Total RNA was extracted using the ZR Fungal/Bacterial RNA MiniPrep kit (R2014, ZymoResearch). Samples were reversed transcribed using TruSeqTM RNA sample preparation Kit (Illumina, California, USA) and sequenced by Illumina HiSeq X Ten (BIOZERON, Shanghai, China).

Clean reads were aligned and processed by BIOZERON biotechnology. Briefly, the reads were aligned to the corresponding reference genomes with HISAT2 (2.0.5) [81]. The reference sequence for Km-V was the FIM1 genome. The reference for Sc-R1 and Sc-R3 was the S288c genome (GenBank assembly: GCA 000146045.2), with the chr1 or chr3 sequences replaced by that of R1 or R3 (see above), respectively. The reference for KS-R1 and KS-R3 combined the FIM1 genome and R1 or R3 respectively. Number of reads covering each gene was counted with featureCounts (1.6.3) in the Subread package [82], with the parameters "-p -C -B -P -O -T 16 -Q 20". Of note, the reads for Km genes were counted based on FIM1 annotations, but the genes

were renamed to be consistent with the nomenclature of a previously published *K. marxianus* DMKU3-1042 genome (GCA_001417885.1). The relationship between FIM1 and DMKU3-1042 labels had been previously published [79].

Differential expression was analyzed with DEseq2 [83]. To examine changes in expression levels before and after chromosomal transfers (Sc vs. KS; Km vs KS), the data were fitted to a model of *count ~ condition,* where *condition* represented a combination between the strain factor (Sc/KS/Km) and the treatment factor (YPD/TM/NaCl). Adjusted p-values for pairwise comparisons between conditions (e.g. Sc-YPD vs. KS-YPD) were derived from FDR-corrected Wald significance tests, with an FDR cutoff of 0.05. Log2 fold changes were shrunken with the ashr method [84]. In this analysis, Sc and Km alleles were treated independently. For Sc, only genes in R1 and R3 were included. Synthetic elements, including *KmURA3*, *HphMX4* and *KanR* cassettes were excluded from the analysis. Genes with an average read count lower than 5 in any condition were removed from the analysis. The removed Sc genes included 6 genes not expressed in Sc (*PAU8*, *YAL067W-A*, *YAR010C*, *YAR035C-A*, *YCL067C*, and *YCL066W*), the 13 genes absent in KS-R3 (see **Results**), and one gene not expressed in either Sc or KS (*YCR040W*), leaving 235 out of 255 genes in the dataset. For Km, 93 genes were filtered out due to low read counts, of which 21 genes had a read count of 0 across all conditions, possibly due to annotation problems, and others showed condition-specific expression. There was a total of 4,857 Km genes after the filters. The median of read counts across conditions was 2,083 for Sc and 1,770 for Km, prior to normalization.

For qPCR, RNA samples were reverse-transcribed using a PrimeScript RT Reagent Kit (RR037A, Takara, China). The qPCR was performed using ChamQ Universal SYBR qPCR Master Mix (Q711-02, Vazyme). The mRNA level was normalized to the average of three housekeeping genes, including *MPE1*, *TRK1*, and *SWC4*. Primers used in qPCR are listed in **Table S6.**

### *Cis* and *trans* effects

The Km orthologs of Sc genes were identified with OrthoDB (v11) [85]. In the case where there were multiple orthologs for one gene, we selected the gene with the highest score in ortholog search in Sequence Similarity DataBase (SSDB) in Kyoto Encyclopedia of Genes and Genomes (KEGG) [86]. The orthologous and Sc-specific genes, essential genes [87], and paralogous genes on R1 and R3 [88] were listed in **Table S7**.

*Cis* and *trans* effects were calculated as previously described [17]. Briefly, read counts were normalized and analyzed using DESeq2. We designated Km alleles in Km-V as kmk, Sc alleles in Sc-R1 or Sc-R3 as scs, Km alleles in hybrids as hyk, and Sc alleles in hybrids as hys. The variables *gb*, *F*, and *allele* were used, where *gb* represents genetic background (Km for kmk, Sc for scs, hybrid-Km for hyk, hybrid-Sc for hys), *F* represents generation (F0 for kmk and scs, F1 for hyk and hys), and *allele* indicates the allele (km for kmk and hyk, sc for scs and hys).

The model "*count* ~ *gb*" was used for testing the significance of *cis*+*trans* and *cis* effect, i.e., contrasts between kmk and scs for *cis* + *trans* effects and between hyk and hys for *cis* effects. P-values were from Wald test followed by an FDR-correction. For testing *trans* effects, another model "*count* ~ *F* + *allele* + *F*:*allele*" was used. Significant *trans* effect was determined by a likelihood ratio test (test = "LRT", reduced = "*F* + *allele*") for testing the effect of the interaction term "*F*:*allele*". Genes with significant *cis* or *trans* effects were defined by a log2-fold change greater than 1 and an FDR-adjusted p-value less than 0.05. YPD, TM and NaCl data were analyzed separately.

The transcriptional response to stress was calculated as the ratio between DESeq2-normalized read counts before and after TM/NaCl treatment. A two-tailed Student's t-test was used to test the significance of stress responses, with a p-value cutoff of 0.05. The contributions of *cis* and *trans* effects to the divergence of transcriptional response under stress were calculated accordingly. The summarized experiment matrix and values of *cis* and *trans* effects are shown in **Table S7**.

**Spot assay and quantification of growth phenotypes under various conditions**

Km-V, Sc-R1, Sc-R3, KS-R1, and KS-R3 were cultured overnight in liquid SD-Ura+GH medium. The cultures were diluted to an $OD_{600}$ of 1.0 and subjected to five serial 5-fold dilutions. These dilutions were spotted on plates using a 48-pin replicator. To evaluate the growth in different carbon sources, we used YP in combination with 2% ethanol, 3% glycerol, or different concentrations of glucose (0.02%, 1%, 3%, and 5%). To evaluate the growth in various nitrogen sources, we replaced 1 g/L sodium glutamate in the SD medium with 1 g/L threonine, 1 g/L serine, or 1.25 g of ammonium sulfate (1/4 N). In the condition of 1/2 AA and 1/2 N, the amino acids supplemented in the SD medium were halved, and 2.5 g/L ammonium sulfate was added. In the plates for chemical treatment, YPD medium was supplemented with 0.08% $H_2O_2$, 60 mM acetic acid (AcOH), 0.4 μg/mL TM, 20 mM DTT, 15 μg/mL 5-FU, 1 M NaCl, 1 M

sorbitol, 20 μg/mL benomyl (BML), 10 μg/mL thiabendazole (TBZ), 0.05 M hydroxyurea (HU), 0.01% methyl methane sulfonate (MMS), 5 μg/mL camptothecin (CPT), or 0.05 μg/mL cycloheximide (CHX). The plates were incubated at 30 ℃ or at other specified temperatures for 1-3 days before the pictures were taken. To quantify growth phenotypes, spot quantification was performed using the 'gitter' package [89] in R, with the dilution factor taken into account. The quantified spot value of a strain under a specific condition was divided by the value of the same strain grown in YPD, to calculate the relative growth value under that condition. Each spot value represents the average of three replicates.

To perform spot assays of cells with plasmids expressing *SPS22*, Sc-R3 was transformed with LHZ1511 or LHZ1512, and Fim-1ΔU was transformed with LHZ1506, LHZ1507, or LHZ1508. Transformants were cultured overnight in SD-Leu medium. The culture was diluted and spotted onto plates with or without 1 M NaCl, as described above.

**Flocculation analysis**

Km-V, KS-R1, and Sc-R1 were cultured overnight in SD-Ura medium. Sc-R1 was transformed with LHZ1509 or LHZ1510. Fim-1ΔU was transformed with LHZ1505. Transformants were cultured overnight in SD-Leu medium. Cells were harvested and washed with $ddH_2O$ and 250 mM EDTA. After two subsequent washes with $ddH_2O$ to ensure complete removal of EDTA, cells equivalent to an $OD_{600}$ of 40 were pelleted and resuspended in 2 mL of $ddH_2O$ in a 15 mL tube. A total of 100 μL of 1 M Tris-HCl (pH 7.5) was added to the cell suspension, followed by 1 min of agitation. The tube was then left undisturbed, and pictures were taken every minute for a total of 5 minutes. Supernatant samples were collected at various time points from the surface for $OD_{600}$ measurement to quantify the flocculation progress.

## References

1. Soucy, S.M., Huang, J., and Gogarten, J.P. (2015). Horizontal gene transfer: building the web of life. Nat. Rev. Genet. *16*, 472–482. https://doi.org/10.1038/nrg3962.

2. Steensels, J., Gallone, B., and Verstrepen, K.J. (2021). Interspecific hybridization as a driver of fungal evolution and adaptation. Nat. Rev. Microbiol. *19*, 485–500. https://doi.org/10.1038/s41579-021-00537-4.

3. Stegemann, S., Keuthe, M., Greiner, S., and Bock, R. (2012). Horizontal transfer of chloroplast genomes between plant species. Proc. Natl. Acad. Sci. *109*, 2434–2438. https://doi.org/10.1073/pnas.1114076109.

4. Ma, L.-J., van der Does, H.C., Borkovich, K.A., Coleman, J.J., Daboussi, M.-J., Di Pietro, A., Dufresne, M., Freitag, M., Grabherr, M., Henrissat, B., et al. (2010). Comparative genomics reveals mobile pathogenicity chromosomes in Fusarium. Nature *464*, 367–373. https://doi.org/10.1038/nature08850.

5. Gibson, B., and Liti, G. (2015). Saccharomyces pastorianus: genomic insights inspiring innovation for industry. Yeast Chichester Engl. *32*, 17–27. https://doi.org/10.1002/yea.3033.

6. Mergoum, M., Singh, P.K., Peña, R.J., Lozano-del Río, A.J., Cooper, K.V., Salmon, D.F., and Gómez Macpherson, H. (2009). Triticale: A "New" Crop with Old Challenges. In Cereals, M. J. Carena, ed. (Springer US), pp. 267–287. https://doi.org/10.1007/978-0-387-72297-9_9.

7. Chen, Z.J. (2013). Genomic and epigenetic insights into the molecular bases of heterosis. Nat. Rev. Genet. *14*, 471–482. https://doi.org/10.1038/nrg3503.

8. Landry, C.R., Hartl, D.L., and Ranz, J.M. (2007). Genome clashes in hybrids: insights from gene expression. Heredity *99*, 483–493. https://doi.org/10.1038/sj.hdy.6801045.

9. Signor, S.A., and Nuzhdin, S.V. (2018). The Evolution of Gene Expression in cis and trans. Trends Genet. TIG *34*, 532–544. https://doi.org/10.1016/j.tig.2018.03.007.

10. Wittkopp, P.J., Haerum, B.K., and Clark, A.G. (2004). Evolutionary changes in cis and trans gene regulation. Nature *430*, 85–88. https://doi.org/10.1038/nature02698.

11. Tirosh, I., Reikhav, S., Levy, A.A., and Barkai, N. (2009). A Yeast Hybrid Provides Insight into the Evolution of Gene Expression Regulation. Science *324*, 659–662. https://doi.org/10.1126/science.1169766.

12. Bullard, J.H., Mostovoy, Y., Dudoit, S., and Brem, R.B. (2010). Polygenic and directional regulatory evolution across pathways in Saccharomyces. Proc. Natl. Acad. Sci. U. S. A. *107*, 5058–5063. https://doi.org/10.1073/pnas.0912959107.

13. Emerson, J.J., Hsieh, L.C., Sung, H.M., Wang, T.Y., Huang, C.J., Lu, H.H.S., Lu, M.Y.J., Wu, S.H., and Li, W.H. (2010). Natural selection on cis and trans regulation in yeasts. Genome Res. *20*, 826–836. https://doi.org/10.1101/gr.101576.109.

14. Fraser, H.B., Levy, S., Chavan, A., Shah, H.B., Perez, J.C., Zhou, Y., Siegal, M.L., and Sinha, H. (2012). Polygenic cis-regulatory adaptation in the evolution of yeast pathogenicity. Genome Res. *22*, 1930–1939. https://doi.org/10.1101/gr.134080.111.

15. Li, X.C., and Fay, J.C. (2017). Cis-regulatory divergence in gene expression between two thermally divergent yeast species. Genome Biol. Evol. *9*, 1120–1129. https://doi.org/10.1093/gbe/evx072.

16. Metzger, B.P.H., Wittkopp, P.J., and Coolon, J.D. (2017). Evolutionary Dynamics of Regulatory Changes Underlying Gene Expression Divergence among Saccharomyces Species. Genome Biol. Evol. *9*, 843–854. https://doi.org/10.1093/gbe/evx035.

17. Krieger, G., Lupo, O., Levy, A.A., and Barkai, N. (2020). Independent evolution of transcript abundance and gene regulatory dynamics. Genome Res. *30*, 1000–1011. https://doi.org/10.1101/gr.261537.120.

18. Gombert, A.K., Madeira, J.V., Cerdán, M.-E., and González-Siso, M.-I. (2016). Kluyveromyces marxianus as a host for heterologous protein synthesis. Appl. Microbiol. Biotechnol. *100*, 6193–6208. https://doi.org/10.1007/s00253-016-7645-y.

19. Bilal, M., Ji, L., Xu, Y., Xu, S., Lin, Y., Iqbal, H.M.N., and Cheng, H. (2022). Bioprospecting Kluyveromyces marxianus as a Robust Host for Industrial Biotechnology. Front. Bioeng. Biotechnol. *10*, 851768. https://doi.org/10.3389/fbioe.2022.851768.

20. Groeneveld, P., Stouthamer, A.H., and Westerhoff, H.V. (2009). Super life – how and why 'cell selection' leads to the fastest-growing eukaryote. FEBS J. *276*, 254–270. https://doi.org/10.1111/j.1742-4658.2008.06778.x.

21. Lertwattanasakul, N., Rodrussamee, N., Suprayogi, Limtong, S., Thanonkeo, P., Kosaka, T., and Yamada, M. (2011). Utilization capability of sucrose, raffinose and inulin and its less-sensitiveness to glucose repression in thermotolerant yeast Kluyveromyces marxianus DMKU 3-1042. AMB Express *1*, 20. https://doi.org/10.1186/2191-0855-1-20.

22. Rodrussamee, N., Lertwattanasakul, N., Hirata, K., Suprayogi, Limtong, S., Kosaka, T., and Yamada, M. (2011). Growth and ethanol fermentation ability on hexose and pentose sugars and glucose effect under various conditions in thermotolerant yeast Kluyveromyces marxianus. Appl. Microbiol. Biotechnol. *90*, 1573–1586. https://doi.org/10.1007/s00253-011-3218-2.

23. Fisk, D.G., Ball, C.A., Dolinski, K., Engel, S.R., Hong, E.L., Issel-Tarver, L., Schwartz, K., Sethuraman, A., Botstein, D., and Michael Cherry, J. (2006). Saccharomyces cerevisiae S288C genome annotation: a working hypothesis. Yeast *23*, 857–865. https://doi.org/10.1002/yea.1400.

24. Witte, V., Grossmann, B., and Emeis, C.C. (1989). Molecular probes for the detection of Kluyveromyces marxianus chromosomal DNA in electrophoretic karyotypes of intergeneric protoplast fusion products. Arch. Microbiol. *152*, 441–446. https://doi.org/10.1007/BF00446926.

25. Albonico, F., B, E., G, P.H., and B, D. (2022). New Saccharomyces cerevisiae-Kluyveromyces marxianus fusant shows enhanced alcoholic fermentation performance. World J. Microbiol. Biotechnol. *38*, 251. https://doi.org/10.1007/s11274-022-03422-1.

26. Fournier, R.E., and Ruddle, F.H. (1977). Microcell-mediated transfer of murine chromosomes into mouse, Chinese hamster, and human somatic cells. Proc. Natl. Acad. Sci. *74*, 319–323. https://doi.org/10.1073/pnas.74.1.319.

27. Fukagawa, T., Nogami, M., Yoshikawa, M., Ikeno, M., Okazaki, T., Takami, Y., Nakayama, T., and Oshimura, M. (2004). Dicer is essential for formation of the heterochromatin structure in vertebrate cells. Nat. Cell Biol. *6*, 784–791. https://doi.org/10.1038/ncb1155.

28. O'Doherty, A., Ruf, S., Mulligan, C., Hildreth, V., Errington, M.L., Cooke, S., Sesay, A., Modino, S., Vanes, L., Hernandez, D., et al. (2005). An aneuploid mouse strain carrying human chromosome 21 with Down syndrome phenotypes. Science *309*, 2033–2037. https://doi.org/10.1126/science.1114535.

29. Wilson, M.D., Barbosa-Morais, N.L., Schmidt, D., Conboy, C.M., Vanes, L., Tybulewicz, V.L.J., Fisher, E.M.C., Tavaré, S., and Odom, D.T. (2008). Species-specific transcription in mice carrying human chromosome 21. Science *322*, 434–438. https://doi.org/10.1126/science.1160930.

30. Lartigue, C., Glass, J.I., Alperovich, N., Pieper, R., Parmar, P.P., Hutchison, C.A., Smith, H.O., and Venter, J.C. (2007). Genome transplantation in bacteria: changing one species to another. Science *317*, 632–638. https://doi.org/10.1126/science.1144622.

31. Shen, X.-X., Opulente, D.A., Kominek, J., Zhou, X., Steenwyk, J.L., Buh, K.V., Haase, M.A.B., Wisecaver, J.H., Wang, M., Doering, D.T., et al. (2018). Tempo and Mode of Genome Evolution in the Budding Yeast Subphylum. Cell *175*, 1533-1545.e20. https://doi.org/10.1016/j.cell.2018.10.023.

32. Kitaoka, M., Smith, O.K., Straight, A.F., and Heald, R. (2022). Molecular conflicts disrupting centromere maintenance contribute to Xenopus hybrid inviability. Curr. Biol. CB *32*, 3939-3951.e6. https://doi.org/10.1016/j.cub.2022.07.037.

33. Kitano, J., and Okude, G. (2024). Causative genes of intrinsic hybrid incompatibility in animals and plants: what we have learned about speciation from the molecular perspective. Evol. J. Linn. Soc. *3*, kzae022. https://doi.org/10.1093/evolinnean/kzae022.

34. Lartigue, C., Vashee, S., Algire, M.A., Chuang, R.-Y., Benders, G.A., Ma, L., Noskov, V.N., Denisova, E.A., Gibson, D.G., Assad-Garcia, N., et al. (2009). Creating bacterial strains from genomes that have been cloned and engineered in yeast. Science *325*, 1693–1696. https://doi.org/10.1126/science.1173759.

35. Minh, B.Q., Schmidt, H.A., Chernomor, O., Schrempf, D., Woodhams, M.D., von Haeseler, A., and Lanfear, R. (2020). IQ-TREE 2: New Models and Efficient Methods for Phylogenetic Inference in the Genomic Era. Mol. Biol. Evol. *37*, 1530–1534. https://doi.org/10.1093/molbev/msaa015.

36. Emms, D.M., and Kelly, S. (2019). OrthoFinder: phylogenetic orthology inference for comparative genomics. Genome Biol. *20*, 238. https://doi.org/10.1186/s13059-019-1832-y.

37. Peska, V., Fajkus, P., Bubeník, M., Brázda, V., Bohálová, N., Dvořáček, V., Fajkus, J., and Garcia, S. (2021). Extraordinary diversity of telomeres, telomerase RNAs and their template regions in Saccharomycetaceae. Sci. Rep. *11*, 12784. https://doi.org/10.1038/s41598-021-92126-x.

38. Shao, Y., Lu, N., Wu, Z., Cai, C., Wang, S., Zhang, L.-L., Zhou, F., Xiao, S., Liu, L., Zeng, X., et al. (2018). Creating a functional single-chromosome yeast. Nature *560*, 331–335. https://doi.org/10.1038/s41586-018-0382-x.

39. Nieduszynski, C.A., Knox, Y., and Donaldson, A.D. (2006). Genome-wide identification of replication origins in yeast by comparative genomics. Genes Dev. *20*, 1874–1879. https://doi.org/10.1101/gad.385306.

40. Noskov, V.N., Chuang, R.-Y., Gibson, D.G., Leem, S.-H., Larionov, V., and Kouprina, N. (2011). Isolation of circular yeast artificial chromosomes for synthetic biology and functional genomics studies. Nat. Protoc. *6*, 89–96. https://doi.org/10.1038/nprot.2010.174.

41. Lyu, Y., Wu, P., Zhou, J., Yu, Y., and Lu, H. (2021). Protoplast transformation of Kluyveromyces marxianus. Biotechnol. J. *16*, e2100122. https://doi.org/10.1002/biot.202100122.

42. Tschumper, G., and Carbon, J. (1986). High frequency excision of Ty elements during transformation of yeast. Nucleic Acids Res. *14*, 2989–3001. https://doi.org/10.1093/nar/14.7.2989.

43. Wu, P., Mo, W., Tian, T., Song, K., Lyu, Y., Ren, H., Zhou, J., Yu, Y., and Lu, H. (2024). Transfer of disulfide bond formation modules via yeast artificial chromosomes promotes the expression of heterologous proteins in Kluyveromyces marxianus. mLife *3*, 129–142. https://doi.org/10.1002/mlf2.12115.

44. Travesa, A., and Wittenberg, C. (2012). Turned on by genotoxic stress. Cell Cycle Georget. Tex *11*, 3145–3146. https://doi.org/10.4161/cc.21587.

45. Walker, G.M., and Basso, T.O. (2020). Mitigating stress in industrial yeasts. Fungal Biol. *124*, 387–397. https://doi.org/10.1016/j.funbio.2019.10.010.

46. Coluccio, A., Bogengruber, E., Conrad, M.N., Dresser, M.E., Briza, P., and Neiman, A.M. (2004). Morphogenetic pathway of spore wall assembly in Saccharomyces cerevisiae. Eukaryot. Cell *3*, 1464–1475. https://doi.org/10.1128/EC.3.6.1464-1475.2004.

47. Chakrabortee, S., Byers, J.S., Jones, S., Garcia, D.M., Bhullar, B., Chang, A., She, R., Lee, L., Fremin, B., Lindquist, S., et al. (2016). Intrinsically Disordered Proteins Drive Emergence and Inheritance of Biological Traits. Cell *167*, 369-381.e12. https://doi.org/10.1016/j.cell.2016.09.017.

48. Soares, E.V. (2011). Flocculation in Saccharomyces cerevisiae: a review. J. Appl. Microbiol. *110*, 1–18. https://doi.org/10.1111/j.1365-2672.2010.04897.x.

49. Teunissen, A.W., and Steensma, H.Y. (1995). Review: the dominant flocculation genes of Saccharomyces cerevisiae constitute a new subtelomeric gene family. Yeast Chichester Engl. *11*, 1001–1013. https://doi.org/10.1002/yea.320111102.

50. Brothers, M., and Rine, J. (2022). Distinguishing between recruitment and spread of silent chromatin structures in Saccharomyces cerevisiae. eLife *11*, e75653. https://doi.org/10.7554/eLife.75653.

51. Sjöstrand, J.O.O., Kegel, A., and Aström, S.U. (2002). Functional diversity of silencers in budding yeasts. Eukaryot. Cell *1*, 548–557. https://doi.org/10.1128/EC.1.4.548-557.2002.

52. Aström, S.U., Kegel, A., Sjöstrand, J.O., and Rine, J. (2000). Kluyveromyces lactis Sir2p regulates cation sensitivity and maintains a specialized chromatin structure at the cryptic alpha-locus. Genetics *156*, 81–91. https://doi.org/10.1093/genetics/156.1.81.

53. De Boer, C.G., and Hughes, T.R. (2012). YeTFaSCo: A database of evaluated yeast transcription factor sequence specificities. Nucleic Acids Res. *40*, 169–179. https://doi.org/10.1093/nar/gkr993.

54. Wittkopp, P.J., Haerum, B.K., and Clark, A.G. (2008). Regulatory changes underlying expression differences within and between Drosophila species. Nat. Genet. *40*, 346–350. https://doi.org/10.1038/ng.77.

55. Escalera-Fanjul, X., Quezada, H., Riego-Ruiz, L., and González, A. (2019). Whole-Genome Duplication and Yeast's Fruitful Way of Life. Trends Genet. TIG *35*, 42–54. https://doi.org/10.1016/j.tig.2018.09.008.

56. Gabaldón, T., and Koonin, E.V. (2013). Functional and evolutionary implications of gene orthology. Nat. Rev. Genet. *14*, 360–366. https://doi.org/10.1038/nrg3456.

57. Pobiega, S., and Marcand, S. (2010). Dicentric breakage at telomere fusions. Genes Dev. *24*, 720–733. https://doi.org/10.1101/gad.571510.

58. Postma, E.D., Dashko, S., van Breemen, L., Taylor Parkins, S.K., van den Broek, M., Daran, J.-M., and Daran-Lapujade, P. (2021). A supernumerary designer chromosome for modular in vivo pathway assembly in Saccharomyces cerevisiae. Nucleic Acids Res. *49*, 1769–1783. https://doi.org/10.1093/nar/gkaa1167.

59. Zhou, J., Zhang, C., Wei, R., Han, M., Wang, S., Yang, K., Zhang, L., Chen, W., Wen, M., Li, C., et al. (2022). Exogenous artificial DNA forms chromatin structure with active transcription in yeast. Sci. China Life Sci. *65*, 851–860. https://doi.org/10.1007/s11427-021-2044-x.

60. Gibson, D.G., Glass, J.I., Lartigue, C., Noskov, V.N., Chuang, R.-Y., Algire, M.A., Benders, G.A., Montague, M.G., Ma, L., Moodie, M.M., et al. (2010). Creation of a bacterial cell controlled by a chemically synthesized genome. Science *329*, 52–56. https://doi.org/10.1126/science.1190719.

61. Fredens, J., Wang, K., de la Torre, D., Funke, L.F.H., Robertson, W.E., Christova, Y., Chia, T., Schmied, W.H., Dunkelmann, D.L., Beránek, V., et al. (2019). Total synthesis of Escherichia coli with a recoded genome. Nature *569*, 514–518. https://doi.org/10.1038/s41586-019-1192-5.

62. Venetz, J.E., Del Medico, L., Wölfle, A., Schächle, P., Bucher, Y., Appert, D., Tschan, F., Flores-Tinoco, C.E., van Kooten, M., Guennoun, R., et al. (2019). Chemical synthesis rewriting of a bacterial genome to achieve design flexibility and biological functionality. Proc. Natl. Acad. Sci. U. S. A. *116*, 8070–8079. https://doi.org/10.1073/pnas.1818259116.

63. Peris, D., Alexander, W.G., Fisher, K.J., Moriarty, R.V., Basuino, M.G., Ubbelohde, E.J., Wrobel, R.L., and Hittinger, C.T. (2020). Synthetic hybrids of six yeast species. Nat. Commun. *11*, 2085. https://doi.org/10.1038/s41467-020-15559-4.

64. Nonklang, S., Ano, A., Abdel-Banat, B.M.A., Saito, Y., Hoshida, H., and Akada, R. (2009). Construction of flocculent Kluyveromyces marxianus strains suitable for high-temperature ethanol fermentation. Biosci. Biotechnol. Biochem. *73*, 1090–1095. https://doi.org/10.1271/bbb.80853.

65. Sasanuma, H., Hirota, K., Fukuda, T., Kakusho, N., Kugou, K., Kawasaki, Y., Shibata, T., Masai, H., and Ohta, K. (2008). Cdc7-dependent phosphorylation of Mer2 facilitates initiation of yeast meiotic recombination. Genes Dev. *22*, 398–410. https://doi.org/10.1101/gad.1626608.

66. Nguyen, T.H., Fleet, G.H., and Rogers, P.L. (1998). Composition of the cell walls of several yeast species. Appl. Microbiol. Biotechnol. *50*, 206–212. https://doi.org/10.1007/s002530051278.

67. Meiklejohn, C.D., Coolon, J.D., Hartl, D.L., and Wittkopp, P.J. (2014). The roles of cis- and trans-regulation in the evolution of regulatory incompatibilities and sexually dimorphic gene expression. Genome Res. *24*, 84–95. https://doi.org/10.1101/gr.156414.113.

68. Guerrero, R.F., Posto, A.L., Moyle, L.C., and Hahn, M.W. (2016). Genome-wide patterns of regulatory divergence revealed by introgression lines. Evol. Int. J. Org. Evol. *70*, 696–706. https://doi.org/10.1111/evo.12875.

69. Gordon, K.L., and Ruvinsky, I. (2012). Tempo and Mode in Evolution of Transcriptional Regulation. PLoS Genet. *8*, e1002432. https://doi.org/10.1371/journal.pgen.1002432.

70. Zhou, J., Zhu, P., Hu, X., Lu, H., and Yu, Y. (2018). Improved secretory expression of lignocellulolytic enzymes in Kluyveromyces marxianus by promoter and signal sequence engineering. Biotechnol. Biofuels *11*, 235. https://doi.org/10.1186/s13068-018-1232-7.

71. Amberg, D.C., Burke, D., Strathern, J.N., and Burke, D. (2005). Methods in yeast genetics: a Cold Spring Harbor Laboratory course manual 2005 ed. (Cold Spring Harbor Laboratory Press).

72. Ren, H., Yin, A., Wu, P., Zhou, H., Zhou, J., Yu, Y., and Lu, H. (2022). Establishment of a Cre-loxP System Based on a Leaky LAC4 Promoter and an Unstable panARS Element in Kluyveromyces marxianus. Microorganisms *10*, 1240. https://doi.org/10.3390/microorganisms10061240.

73. Antunes, D.F., de Souza Junior, C.G., and de Morais Junior, M.A. (2000). A simple and rapid method for lithium acetate-mediated transformation of Kluyveromyces marxianus cells. World J. Microbiol. Biotechnol. *16*, 653–654. https://doi.org/10.1023/A:1008984403732.

74. Gietz, R.D., and Schiestl, R.H. (2007). Large-scale high-efficiency yeast transformation using the LiAc/SS carrier DNA/PEG method. Nat. Protoc. *2*, 38–41. https://doi.org/10.1038/nprot.2007.16.

75. Shi, T., Zeng, J., Zhou, J., Yu, Y., and Lu, H. (2022). Correlation Between Improved Mating Efficiency and Weakened Scaffold-Kinase Interaction in the Mating Pheromone Response Pathway Revealed by Interspecies Complementation. Front. Microbiol. *13*, 865829. https://doi.org/10.3389/fmicb.2022.865829.

76. Shao, Y., Lu, N., Qin, Z., and Xue, X. (2018). CRISPR-Cas9 Facilitated Multiple-Chromosome Fusion in Saccharomyces cerevisiae. ACS Synth. Biol. *7*, 2706–2708. https://doi.org/10.1021/acssynbio.8b00397.

77. Li, H., and Durbin, R. (2009). Fast and accurate short read alignment with Burrows-Wheeler transform. Bioinforma. Oxf. Engl. *25*, 1754–1760. https://doi.org/10.1093/bioinformatics/btp324.

78. McKenna, A., Hanna, M., Banks, E., Sivachenko, A., Cibulskis, K., Kernytsky, A., Garimella, K., Altshuler, D., Gabriel, S., Daly, M., et al. (2010). The Genome Analysis Toolkit: a MapReduce framework for analyzing next-generation DNA sequencing data. Genome Res. *20*, 1297–1303. https://doi.org/10.1101/gr.107524.110.

79. Yu, Y., Mo, W., Ren, H., Yang, X., Lu, W., Luo, T., Zeng, J., Zhou, J., Qi, J., and Lu, H. (2021). Comparative Genomic and Transcriptomic Analysis Reveals Specific Features of Gene Regulation in Kluyveromyces marxianus. Front. Microbiol. *12*, 598060. https://doi.org/10.3389/fmicb.2021.598060.

80. Danecek, P., Auton, A., Abecasis, G., Albers, C.A., Banks, E., DePristo, M.A., Handsaker, R.E., Lunter, G., Marth, G.T., Sherry, S.T., et al. (2011). The variant call format and VCFtools. Bioinformatics *27*, 2156–2158. https://doi.org/10.1093/bioinformatics/btr330.

81. Kim, D., Paggi, J.M., Park, C., Bennett, C., and Salzberg, S.L. (2019). Graph-based genome alignment and genotyping with HISAT2 and HISAT-genotype. Nat. Biotechnol. *37*, 907–915. https://doi.org/10.1038/s41587-019-0201-4.

82. Liao, Y., Smyth, G.K., and Shi, W. (2014). featureCounts: an efficient general purpose program for assigning sequence reads to genomic features. Bioinforma. Oxf. Engl. *30*, 923–930. https://doi.org/10.1093/bioinformatics/btt656.

83. Love, M.I., Huber, W., and Anders, S. (2014). Moderated estimation of fold change and dispersion for RNA-seq data with DESeq2. Genome Biol. *15*, 550. https://doi.org/10.1186/s13059-014-0550-8.

84. Stephens, M. (2017). False discovery rates: a new deal. Biostat. Oxf. Engl. *18*, 275–294. https://doi.org/10.1093/biostatistics/kxw041.

85. Kuznetsov, D., Tegenfeldt, F., Manni, M., Seppey, M., Berkeley, M., Kriventseva, E.V., and Zdobnov, E.M. (2023). OrthoDB v11: annotation of orthologs in the widest sampling of organismal diversity. Nucleic Acids Res. *51*, D445–D451. https://doi.org/10.1093/nar/gkac998.

86. Kanehisa, M., Furumichi, M., Sato, Y., Matsuura, Y., and Ishiguro-Watanabe, M. (2025). KEGG: biological systems database as a model of the real world. Nucleic Acids Res. *53*, D672–D677. https://doi.org/10.1093/nar/gkae909.

87. Lai, H.-Y., Yu, Y.-H., Jhou, Y.-T., Liao, C.-W., and Leu, J.-Y. (2023). Multiple intermolecular interactions facilitate rapid evolution of essential genes. Nat. Ecol. Evol. *7*, 745–755. https://doi.org/10.1038/s41559-023-02029-5.

88. Byrne, K.P., and Wolfe, K.H. (2005). The Yeast Gene Order Browser: combining curated homology and syntenic context reveals gene fate in polyploid species. Genome Res. *15*, 1456–1461. https://doi.org/10.1101/gr.3672305.

89. Wagih, O., and Parts, L. (2014). gitter: a robust and accurate method for quantification of colony sizes from plate images. G3 Bethesda Md *4*, 547–552. https://doi.org/10.1534/g3.113.009431.

## Acknowledgments

## Funding:

Science and Technology Research Program of Shanghai 24ZR1406500 (YY)

National Key Research and Development Program of China grant 2021YFA0910603 (YY)

National Key Research and Development Program of China grant 2022YFC2106201 (JZ)

National Key Research and Development Program of China grant 2021YFA0910601 (HL)

Science and Technology Research Program of Shanghai grant 2023ZX01 (HL)

Open Fund of State Key Laboratory of Genetic Engineering grant SKLGE-2318 (YY)
The Fundamental Research Funds for the Central Universities (XCL)
Young Scientists Fund of the National Natural Science Foundation of China, grant #32400495 (XCL).

**Author contributions:**

Conceptualization: HL, YY
Methodology: HL, YY, YL
Investigation: YL, KS, JZ, HC, XCL
Writing—original draft: YL, YY
Writing—review & editing: YL, YY, YW, XH, XCL

**Competing interests:**

Authors declare that they have no competing interests.

**Data and materials availability:**

DNA-seq and RNA-seq data are available in the NCBI. (https://dataview.ncbi.nlm.nih.gov/object/PRJNA1102743?reviewer=98okerqm686mrj3ddq79r4l18u)

**Supplementary Materials**

Fig. S1. Transformation efficiency and stability of plasmids containing different combinations of *ARS* and *CEN* from Km and Sc.
Fig. S2. Zygotes formed between Km cells and between Sc cells.
Fig. S3. Growth of Sc-R1 and Sc-R3.
Fig. S4. Identification of a 29 kb deletion in R3.
Fig. S5. PFGE of Km chromosomes.
Fig. S6. Growth of hybrids and their parental strains under various conditions.
Fig. S7. Growth of KS-R1 and KS-R3 after loss of Sc chromosomes.
Fig. S8. Flocculation of Km and KS-R1ΔR1.
Fig. S9. Expression differences along R1 and R3 chromosomes in TM and NaCl conditions.
Fig. S10. Proportion of genes exhibiting conserved and diverged regulation in stress conditions.
File S1. Donors used in the engineering of Sc chr1 and chr3.

Table S1. Strains used in this study.

Table S2. Plasmids used in this study, and sequences of LHZ626, LHZ1495 and pRS425-Cas9-2xSapI.

Table S3. SNPs and INDELs on Km chromosomes of R1&R3.

Table S4. Read counts of R1 and R3 genes, with reference sequences for R1 and R3.

Table S5. Differentially expressed Km genes in KS-R1 and KS-R3.

Table S6. Primers used in this study.

Table S7. Homologous, Sc-specific, essential and paralogous genes on R1 and R3, and their cis and trans effects under 3 conditions.